Centennial-scale age offsets of plant wax *n*-alkanes in Adirondack lake sediments

Erika J. Freimuth[a], Aaron F. Diefendorf[a, *], Thomas V. Lowell[a], Anna K. Schartman[b], Joshua D. Landis[c], Alexander K. Stewart[d], and Benjamin R. Bates[a]

[a] Department of Geology, University of Cincinnati, Cincinnati, OH 45221, USA

[b] Department of Ocean Sciences, University of California, Santa Cruz, Santa Cruz, CA 95064, USA

[c] Department of Earth Sciences, Dartmouth College, Hanover, NH 03755-3571, USA

[d] Department of Geology, St. Lawrence University, Canton, NY 13617, USA

[*]Corresponding Author. Tel. : +1-513-556-3787.

E-mail address: aaron.diefendorf@uc.edu (A.F. Diefendorf).

Keywords: plant biomarkers, radiocarbon, forests, soils, temperate lakes, carbon storage, terrestrial carbon

ABSTRACT

Lacustrine sediments have the potential to preserve paleoenvironmental proxies such as terrestrial plant waxes at high temporal resolution. The temporal fidelity of plant wax records, however, can be up to several thousand years older than the corresponding sediment, based on compound-specific radiocarbon (^{14}C) analysis. Unfortunately, the factors controlling ^{14}C age offsets between plant waxes and sediments are not well understood. The aims of this study are to quantify and compare plant wax *n*-alkane ^{14}C age offsets among lakes within the same region, and to determine if drainage and lake basin differences (e.g., size, relief, drainage basin morphology, fluvial inputs) influence these offsets. We collected sediments from five lakes in the Adirondack Mountains, NY, USA that lack petrogenic sources of *n*-alkanes, and range in drainage basin characteristics. Sediment age models were constructed for each lake using a combination of sediment ^{210}Pb, ^{137}Cs, and macrofossil ^{14}C ages, and compared to ^{14}C ages of long-chain (*n*-C_{27}, *n*-C_{29}, *n*-C_{31}) alkanes sampled from Holocene and Late Glacial aged sediments. The *n*-alkane ^{14}C $age_{initial}$ is a measure of the age offset in *n*-alkanes relative to the sediment they are deposited in. Across all lakes, the *n*-alkane ^{14}C $age_{initial}$ ranged from penecontemporaneous to 2,440 ^{14}C yr. This oldest *n*-alkane ^{14}C $age_{initial}$ is significantly outside the distribution of all other samples; when excluded, the overall mean *n*-alkane ^{14}C $age_{initial}$ was 400 ± 255 ^{14}C yr (n = 23). The largest *n*-alkane ^{14}C $age_{initial}$ values were observed in the last 1 cal kyr BP (565 ± 180 ^{14}C yr (1σ), n = 12)) compared to sediments deposited between 1 and 13 cal kyr BP (220 ± 195 ^{14}C yr (1σ), n = 11)). These age offsets develop early after initial lake basin sedimentation and follow a similar pattern in all of the lakes despite differences in lake basin and catchment size, relief, and geomorphology. We speculate that ^{14}C age offsets occur due to reworking of older *n*-alkanes stored in drainage basin sediments and soils and this mechanism is most effective in the last ~1 kyr. Regardless, lakes in temperate forested metamorphic bedrock terrains have relatively small and stable *n*-alkane age offsets compared with lakes with extensive catchment soils or anthropogenic

42 disturbance. By targeting lakes with minimal catchment soils, age offsets may be reduced, thereby
43 minimizing attenuation or age distortion of climate signals in plant wax isotopic records.

1. INTRODUCTION

Lake sediment records of plant wax molecules (such as long chain *n*-alkanes; $\geq C_{27}$) and their isotopic compositions are increasingly used to understand past changes in terrestrial ecosystems and hydroclimate. An underlying assumption of these records is that *n*-alkanes are penecontemporaneous with the age of the sediment from which *n*-alkanes are extracted. However, compound-specific radiocarbon analyses (CSRA) in fluvial and marine systems indicate that plant wax age can lag behind sediment age by centuries to millennia. This age difference, or offset, is thought to reflect incorporation of older plant waxes from soils or from petrogenic sources (e.g., Eglinton et al., 1997; Pearson and Eglinton, 2000; Pearson et al., 2001; Smittenberg et al., 2004; Kusch et al., 2010). Controls on the prevalence and extent of plant wax age offsets relative to sediments are not fully understood and likely include mixing from multiple sources and transport mechanisms.

Plant wax *n*-alkanes are transported to lake sediments through three main mechanisms. The first mechanism is ablation from leaf surfaces, where *n*-alkanes are transported as aerosols, and then deposited over lakes through dry particle settling or wet precipitation scavenging. This transport mechanism is likely to result in minimal (< 1 year) age offsets (Meyers and Kites, 1982; Nelson et al., 2017; Nelson et al., 2018). The second mechanism is the transport of *n*-alkanes on leaves through litterfall. This litter is transported to lakes directly by wind or accumulates on the forest floor and is then remobilized by fluvial transport soon (within several years) after litterfall occurs. Finally, *n*-alkanes enter soils where they can be stored for long periods of time (100s to 1,000s years) before remobilization by soil erosion (e.g., Diefendorf and Freimuth, 2017). These transport processes operate on different spatial and temporal scales and can thus influence the magnitude of *n*-alkane age offsets. The relative contribution of these processes is not fully understood and may vary across depositional settings; however, recent studies suggest some general patterns.

Aerosol *n*-alkanes, the first mechanism, likely integrate plant wax *n*-alkane sources at regional scales (10s to 100s of km) in temperate forests (Nelson et al., 2017; Nelson et al., 2018), in prairie

ecosystems (Conte et al., 2003), and in both arid and humid subtropical regions (Gao et al., 2014). Observations indicate that aerosol *n*-alkane concentrations are highest during the spring when leaves emerge (Doskey, 2000; Nelson et al., 2017), and lake sediment *n*-alkanes reflect the δ^2H signatures of springtime aerosol *n*-alkanes, suggesting rapid deposition of aerosol *n*-alkanes following spring leaf emergence, at least in temperate settings (Freimuth et al., 2017; Nelson et al., 2018).

The transport of *n*-alkanes via leaf litter, the second mechanism, to lake sediments by wind and through surface waters is limited spatially to the drainage basin, with woody vegetation and leaves being preferentially transported to lake sediments (McQueen, 1969; Drake and Burrows, 1980; Spicer and Wolfe, 1987; Greenwood, 1991). Collection of airborne litterfall in autumn using lake surface and bottom traps (Gasith and Hosier, 1976) suggests annual fluxes of leaves to lakes are by far greatest in the autumn. Additionally, litterfall in lakes is greatest with high ratios of shoreline perimeter to lake area (Jordan and Likens, 1975; Gasith and Hosier, 1976; Casper et al., 1985) in forested catchments. Isotopic comparisons of plant waxes from lake sediments and catchment vegetation suggest that *n*-alkane input from angiosperm trees dominates long-chain *n*-alkanes (C_{27} through C_{31}) in lacustrine sediments (Cranwell et al., 1987; Sachse et al., 2006; Diefendorf et al., 2011; Sachse et al., 2012; Diefendorf and Freimuth, 2017; Freimuth et al., 2017; Freimuth et al., 2019).

Remobilization of old plant waxes from soils and transport into lake sediments, the third mechanism, can result in centennial to millennial scale ^{14}C age offsets (Douglas et al., 2014; Gierga et al., 2016; Douglas et al., 2018; Bowen et al., 2019; Haas et al., 2020). The extent of this ^{14}C age offset potentially correlates with various catchment-specific factors such as catchment and lake size, soil development, landscape erosion/stabilization, lake hydrology (e.g., with and without outlets), and changes in aridity (Uchikawa et al., 2008; Bray et al., 2014; Douglas et al., 2014; Gierga et al., 2016; Bowen et al., 2019). For example, catchment size, relief, and climate were identified in the Black Sea (Kusch et al., 2010); permafrost coverage and temperature in the Arctic (Feng et al., 2013); catchment size and precipitation around Central American lakes (Conte et al., 2003; Douglas et al., 2014); and wetland cover and hydrology in the Congo River drainage basin (Schefuß et al., 2016). Globally, carbon turnover times

in terrestrial ecosystems generally increase with latitude, ranging from mean carbon turnover time of 15 yr for tropical forests to 65 yr in tundra ecosystems; temperate forests have a mean carbon turnover time of 23 yr (Carvalhais et al., 2014). In addition to climatic and depositional controls, anthropogenic land use change influences the transfer of plant waxes that are potentially 1000s of ^{14}C years older into river systems (French et al., 2018) and in lake systems (Gierga et al., 2016; Douglas et al., 2018). Observations from lacustrine, deltaic and marine sediments suggest that a large proportion (~75 to 80%) of sedimentary waxes are likely derived from an 'old' pool of compounds stored on millennial timescales (Douglas et al., 2014; French et al., 2018; Vonk et al., 2019).

To date, relatively few studies have applied radiocarbon dating of plant waxes to lake sediments and therefore the prevalence and mechanistic controls on plant wax age offsets in lake sediment records is poorly understood, especially when plant waxes are sought as a high temporal-resolution proxy. Inputs of long-stored *n*-alkanes into lake sediments has the potential to distort the magnitude and timing of isotopic shifts in plant wax proxy records relative to the original paleoclimate or paleovegetation signals they reflect. This distortion will depend on the age and relative contribution of old plant wax, the amount of reworking, and the isotopic composition of this reworked pool.

Here, we explore ^{14}C age offsets of plant wax *n*-alkanes (C_{27}, C_{29}, C_{31}) in five lakes located in the Adirondack Mountains in NY, USA to test the following hypothesis: if the transport of terrestrial plant wax into lake sediments is controlled primarily by basin-specific geomorphic factors, then sedimentary *n*-alkane age offsets would be expected to vary systematically among lakes with varying basin and catchment size, relief, fluvial inputs and soil development. These five lakes were glacially formed in metamorphic rocks and have had active sedimentation since the Late Glacial. Logging in the region began in the 1800s and was very selective by location and tree species and should not be confused with full deforestation as was done for farming (Fox, 1902; Defebaugh, 1906; McMartin, 1994). Given the possible climatic, anthropogenic and morphological controls on *n*-alkane ^{14}C age offsets and inputs of older reworked *n*-alkanes to lake sediments, we hold climatic controls approximately constant by sampling lakes within the same region (Fig. 1) with similar bedrock and lacking a petrogenic *n*-alkane

source. Lakes range in drainage basin morphology, including size, relief, soil storage, fluvial inputs, and overall complexity. We briefly discuss the effect that *n*-alkane age offsets have on carbon and hydrogen isotopic records generated from plant wax *n*-alkanes for paleoclimate applications.

2. METHODS

2.1. Study area

Sediments were collected from five lakes in the Adirondack Mountains, NY, USA (Fig. 1 and 2, Table 1). The Adirondacks are underlain by metamorphic rocks of Middle Proterozoic age. These rocks predate land plants by > 1 Ga and are significantly metamorphosized (heat and pressure), thus removing petrogenic *n*-alkane sources. Climate conditions are similar at each of the sampled lakes, with mean annual precipitation of 110 cm/yr and mean annual temperatures of 5 ºC (PRISM, 2020). The Adirondacks were forested between ~11.9 to ~9.6 cal kyr BP and modern vegetation assemblages were established beginning around 2.0 cal kyr BP (Overpeck, 1985; Whitehead et al., 1989; Whitehead and Jackson, 1990; Jackson and Whitehead, 1991; Lavoie et al., 2015). The current vegetation assemblages in the drainage basins are mixed conifer-angiosperm forests. Pollen records indicate that a dominance of herbs at all elevations from ice retreat until approximately 12 cal yr BP, when the first tree taxon (*Picea*) is observed (Whitehead et al., 1989). This provides an approximate maximum age for relic long-chain plant wax *n*-alkanes that can be remobilized from catchment soils. Detailed drainage and lake basin characteristics and morphology are described in Section 3.1 and Electronic Annex (EA) Supplemental Note.

2.2. Basin analysis and geophysics

In order to evaluate the geomorphology and soil properties of the lake catchments, high resolution Lidar data (Lidar Point Cloud, ~0.35 – 0.70) produced by the United States Geological Survey was downloaded from The National Map (https://viewer.nationalmap.gov/basic/) in January 2019 and imported into the geographical information system open-source software QGIS for catchment delineation. Catchments were defined based upon delineating the local topographic divides thus capturing some subtleties not possible with automated processing. Freimuth et al. (2020) reported lake catchment physical information using 30 m digital elevation models). In this study, we re-evaluated catchment size using the higher resolution Lidar dataset because of its increased spatial resolution (Table 1). The soil types and properties atop the bedrock were extracted from the Web Soil Survey (https://websoilsurvey.sc.egov.usda.gov; April 20th, 2020).

At Moose Pond, sediment hardness was measured using a consumer grade broad sonar system (Fig. EA1). A seismic profile (Fig. EA2; transect indicated in Fig. EA1) was acquired with a 10 Khz Stratibox subbottom profiler operating in energy mode with 8-bit sampling. The raw image was processed to map the entire energy returns onto a full grayscale image.

2.3. Sediment collection

Sediments were collected from the deepest part of each lake in October 2016 and January 2017, with the exception of Moose Pond which was cored near the deepest point, at 20 m water depth (Table 1; Fig. 2). The upper ~1.2 m of sediment, including the sediment-water interface, was collected from each lake using a square-rod piston corer with a 1.5 m drive length polycarbonate barrel ("Bolivia corer"). Headspace water was drained and the void was trimmed and filled with 2-5 cm of cellulose sponges (free of extractable lipids) or with sodium polyacrylate before capping. In addition, East Pine, Heart and Moose lakes were cored until refusal (~6-7 m) using a Livingstone square-rod piston corer. All cores were stored at 4 ºC until splitting and analysis.

2.4. Sediment chronology

Age models for sediment cores from all five lake basins were created using a combination of ^{14}C ages of organic terrestrial macrofossils and sediment ^{210}Pb ages. In order to generate the ^{210}Pb chronology, all Bolivia cores were sampled from one half of each core in intervals of 0.5 – 2 cm until excess ^{210}Pb was no longer measurable. Chronologies were then constructed with ^{210}Pb dates and the Constant Rate of Supply (CRS) model following Appleby and Oldfield (1978) at the Dartmouth Short-Lived Isotope Lab, in Hanover, New Hampshire. Gamma spectrometry conducted with Canberra well-type and broad-energy intrinsic Ge detectors was used to measure total ^{210}Pb for each depth interval ($^{210}Pb_T$). The CRS model requires the calculation of the atmospheric, or excess, ^{210}Pb component ($^{210}Pb_{xs}$). This was accomplished by subtracting the uniform supported ^{210}Pb activity for each core from the measured $^{210}Pb_T$. The convergence of the $^{210}Pb_T$ asymptote with the measured ^{226}Ra, ^{214}Pb and ^{214}Bi activities for each core, estimated as the variance-weighted mean of these measures, was used for the supported ^{210}Pb activity. Analytical and age model uncertainties were propagated following Landis et al. (2012) and Binford (1990) respectively, and ages are reported in Gregorian Calendar years. The sediment lake chronologies based on the ^{210}Pb dates are reported in Figure EA3 and Data Table 1 (models for Heart Lake and Moose Pond were previously reported in Schartman et al. (2020)). Additionally, the fission product ^{137}Cs was measured to corroborate estimated ^{210}Pb ages with the 1963 atmospheric 'bomb-spike' (Fig. A3; Data Table 1). Following ^{210}Pb dating, two 'pre-bomb' intervals were sub-sampled for CSRA from each of the Bolivia cores (n = 10). The 'pre-bomb' CSRA samples were taken from sediment dated between 1750-1915 to ensure that the samples predated nuclear bomb testing to avoid the 'bomb-spike' in ^{14}C.

To extend the sediment chronology, samples were collected for radiocarbon analysis. One terrestrial macrofossil sample was collected near the base of each Bolivia sediment core section, excepting Wolf Pond where two samples were taken (Table 2). Additionally, terrestrial macrofossils were also collected from the Livingston sediment cores at East Pine Pond (n = 3), Moose Pond (n = 8) and Heart Lake (n = 9). Briefly, all samples were removed from cores and rinsed with DI water under a

stereomicroscope, and dried at 60°C. Before dating, samples were pre-treated at NOSAMS using a sequence of 10% HCl (1 h at 60 ºC), 2% NaOH (1 h at 60 ºC, repeated until solution was free of color), and 10% HCl (1 h at 60 ºC), with three rinses with DI water after each acid or base treatment. Pre-treated samples were filtered, dried, weighed and dated by accelerator mass spectrometry (AMS) at the National Ocean Sciences Accelerator Mass Spectrometry (NOSAMS) facility (Table 2).

We employed Bayesian age-depth modeling techniques (Bacon v2.2; Blaauw and Christen, 2011) integrating both ^{210}Pb and ^{14}C ages from the Bolivia (and where available, the Livingston) cores in order to generate sediment chronologies for each lake basin (Fig. 3 and EA4). The Bacon age-depth model requires inputs related to four different parameters prior to each model run, two of which are related to the accumulation rate directly, the accumulation mean (acc.mean) and accumulation shape (acc.shape) and two related to the model memory of accumulation rate, memory mean (mem.mean) and memory strength (mem.strength). We chose to accept the default values for all inputs, excepting the accumulation mean at Debar Pond, which was set to a value of 2 (Fig. EA4). If the default accumulation mean is accepted for Debar Pond, the resulting model is unstable with large confidence intervals. This is likely caused by the single radiocarbon sample from the base of the Debar Pond's Bolivia sediment core having a radiocarbon age < 500 years. After generating the age-depth models, we assigned ages to the CSRA samples based on their sampling depth within the sediment cores. This necessitated that we extrapolate the age-depth relationship for Debar Pond and East Pine Pond past the lowest radiocarbon sample depth, but by no more than 6 cm. Final age-depth models are shown in Figure 3 and the model original output are included in Figure EA4. The Heart Lake and Moose Pond models are first described in Schartman et al. (2020) and are included here. Lake sedimentation rates are plotted in Figure EA5. We report ages in cal yr BP (before 1950) and ^{14}C yr BP. Following convention, ages are rounded only after calculations, error propagations, and statistical analyses and are reported throughout the text and in Table 2. Unrounded values are reported in Table EA2 and the archived Data Table 2 (Stuiver and Polach, 1977; Millard, 2014).

226 **2.5. Grain size analysis**

227

228 Grain size analysis was determined following previously established methods (Gray et al., 2010).
229 Organic matter was removed using 30% H_2O_2 at room temperature for 24 h followed by three repeat 24 h
230 treatments with 30% H_2O_2 at 70 ºC. Biogenic silica was then removed using 1 M NaOH at 60 ºC for 6 h.
231 Lastly, carbonates were removed using 1 M HCl at room temperature. Sediments were freeze dried and
232 weighed to determine the percent lithics. Grain size particle distribution was determined as an average of
233 three measurements per sample using a Beckman-Coulter LS230 laser diffraction particle size analyzer.
234 Grain size was previously reported in Freimuth et al. (2020) and Schartman et al. (2020) and is rereported
235 here for comparison between all lakes reported in this study (Fig. EA6).

236

237 **2.6. Sample preparation for compound-specific radiocarbon analysis**

238

239 A total of 24 sediment sub-samples were taken for CSRA (Fig. 3). These sub-samples were
240 centered either on ^{210}Pb-dated intervals in Bolivia cores (n = 2 samples per lake; 10 total) or on
241 macrofossils in Bolivia and Livingstone cores from Debar Pond (n = 1), East Pine Pond (n = 3), Heart
242 Lake (n = 5), Moose Pond (n = 4), and Wolf Pond (n = 1). Sediment interval widths for CSRA ranged
243 from 2 to 10 cm (mean = 4.7 cm; n = 24) and were kept as small as possible to minimize the integrated
244 time represented in the sample (see Section 3.2 and Table EA2) while also collecting sufficient long-chain
245 *n*-alkanes for CSRA analysis.

246 Sediment samples for CSRA were freeze-dried, homogenized, and then extracted using
247 accelerated solvent extraction (ASE; Dionex 350) with 9:1 DCM/MeOH (v/v) using three extraction
248 cycles at 100 ºC. The TLE was subsequently saponified with 0.5 N KOH in MeOH/H_2O (3:1, v/v)
249 following Freimuth et al. (2020). After re-extraction with hexanes/DCM, neutral and acid fractions were
250 separated using DCM/IPA (2:1, v/v) and 4% formic acid in diethyl ether, respectively, over aminopropyl-
251 bonded silica gel. The neutral fraction was then separated into aliphatic and polar fractions using activated

252 Al_2O_3 columns. Saturated compounds were separated from the aliphatic fraction over 5% silver
253 impregnated silica gel with hexanes. Two rounds of urea adduction were used to separate *n*-alkanes from
254 branched and cyclic compounds. The purity of *n*-alkanes was confirmed and their abundance determined
255 by gas chromatography (GC)-mass spectrometry (MS)/flame ionization detection (FID) at the University
256 of Cincinnati following the methods of Freimuth et al. (2020).
257 Long-chain *n*-C_{27}, *n*-C_{29} and *n*-C_{31} alkanes were isolated and collected together in a single
258 fraction by preparative capillary gas chromatography (PCGC) at the National Ocean Sciences Accelerator
259 Mass Spectrometry (NOSAMS) laboratory. The isolated compounds were collected in a pre-combusted
260 glass trap, which was rinsed with hexanes into a collection vial. Each fraction-collected sample was
261 purified using silica gel columns and purity checked by GC-FID before transferring in *n*-pentane to a pre-
262 combusted (900 ºC for 3 hr) quartz tube and solvent was completely evaporated with nitrogen. Pre-
263 combusted cupric oxide and silver chips were added before flame-sealing and combusting at 850 ˚C for 5
264 hr. The resulting CO_2 was quantified and purified on a vacuum line before reducing to graphite for ^{14}C
265 analysis by AMS.
266 The reported ^{14}C data from NOSAMS were corrected for graphitization and AMS instrument
267 blank. To account for the PCGC/combustion blank, we used the blank size and established fraction
268 modern (Fm) on the NOSAMS PCGC system (0.4317 ± 0.08). For each sample, the blank size was
269 calculated based on sample size and trapping time, and ranged from 0.41 to 0.60 (mean: 0.5) µg C (Table
270 EA2). The total trapped *n*-alkanes (*n*-C_{27}, *n*-C_{29}, and *n*-C_{31}) for each sample ranged from 30.8 to 132.9 µg
271 C (median = 63.7, n = 24; Table EA2), of which the blank contributed between 0.5 to 1.6% of the total
272 trapped sample mass (median = 0.7%, n = 24).
273
274 **2.7. *n*-Alkane ^{14}C ages and age offset calculations**
275
276 *n*-Alkane age offsets relative to sediment age are calculated in two ways (Table EA2) for
277 comparisons to previous studies. First, following Schefuß et al. (2016), we used the measured Fm of the

combined *n*-C_{27}, *n*-C_{29} and *n*-C_{31} alkanes to calculate the initial *n*-alkane $\Delta^{14}C$ at the time of sediment deposition ($\Delta^{14}C_{initial}$) according to Eq. 1.

$$n\text{-Alkane } \Delta^{14}C_{initial} = (Fm\ e^{\lambda t} - 1) \quad \text{(Eq. 1)}$$

In Eq. 1, λ is the ^{14}C decay constant (1/8,267 yr^{-1}) and *t* is the time of deposition in calendar years BP. $\Delta^{14}C_{initial}$ is reported in ‰. Based on the sediment age, as determined from the sediment age models, we determined the $\Delta^{14}C_{atm}$ values of the past atmosphere using (Reimer et al., 2013). The $\Delta^{14}C_{initial}$ errors were then calculated by propagating the uncertainties in the blank corrected Fm (1σ) and the uncertainty in the sediment age (t) as determined from the BACON sediment age model (95% confidence interval; this overestimates error). Error propagation was completed using the Monte Carlo method of error propagation with 10,000 simulations (Anderson, 1976). $\Delta^{14}C_{initial}$ was then used to calculate $\Delta\Delta^{14}C_{initial}$, which is the $\Delta^{14}C$ difference between the *n*-alkanes $\Delta^{14}C_{initial}$ and the past atmosphere $\Delta^{14}C_{atm}$ using Eq. 2.

$$n\text{-Alkane } \Delta\Delta^{14}C_{initial} = \Delta^{14}C_{initial} - \Delta^{14}C_{atm} \quad \text{(Eq. 2)}$$

The $\Delta\Delta^{14}C_{initial}$ error was determined by propagating the uncertainty determined for the $\Delta^{14}C_{initial}$ in Eq 1. and the uncertainties reported in (Reimer et al., 2013). The *n*-alkane $\Delta^{14}C_{initial}$ values were then converted to the *n*-alkane apparent initial ages in ^{14}C years using Eq. 3 and provides the ^{14}C age offset of the *n*-alkanes at the time of sediment deposition. The $^{14}C\ age_{initial}$ represents the average *n*-alkane ^{14}C age at the time of deposition in the lake sediment. The error in *n*-alkane $^{14}C\ age_{initial}$ was also determined by propagating the uncertainties in $\Delta^{14}C_{initial}$ and in $\Delta^{14}C_{atm}$.

$$n\text{-Alkane } ^{14}C\ age_{initial} = -8{,}033 \times \ln[(1+\Delta^{14}C_{initial}/1{,}000)/(1+\Delta^{14}C_{atm}/1{,}000)] \quad \text{(Eq. 3)}$$

303 The second approach for calculating *n*-alkane age offsets utilized the mean transit time of *n*-
304 alkanes (MTT_{wax}; Table EA2), which is the age difference between *n*-alkane age (cal yr BP) and the age
305 of the sediment (cal yr BP). MTT follows the approach of Douglas et al. (2018) and is presented here for
306 comparison with data synthesized in that study. *n*-Alkane calibrated ages were determined with Calib 7.10
307 using the intCal 13 calibration curve (Stuiver and Reimer, 1993; Reimer et al., 2013) and errors
308 propagated with the uncertainties of the calibrated *n*-alkane ages and the sediment ages.
309 Statistical analyses were completed using JMP Pro 14.0 (SAS, Cary, USA) and Monte Carlo error
310 propagation was completed with Matlab (R2020A, Mathworks, Natick, USA).
311
312 **3. RESULTS**
313
314 **3.1. Basin geography and geomorphology**
315
316 The general geography of the lakes and the surrounding drainage basins (Table 1) may impact
317 plant wax *n*-alkane transport to lakes and accumulation in sediment, thereby influencing *n*-alkane age
318 offsets in lake sediments. Below are descriptions of the five catchment areas with a focus on the potential
319 of the drainage basin to supply a reservoir of older plant wax *n*-alkanes from sediments and soils for
320 reworking into the lake basin. For detailed site descriptions, see EA Supplemental Note. This reservoir
321 depends on both the potential to store and to deliver old sediment and *n*-alkanes to the lake basin. We
322 would not expect any reservoir effect if the basin were purely barren bedrock, assuming that soils are the
323 primary source of old plant waxes.
324 Heart Lake (Fig. 2a) is bound on the north and southwest sides by steep bedrock and on the east
325 side by glacial drift. The drainage soils are limited to the lower slopes and are comprised of lodgment tills
326 that are well drained with high runoff potential. The drift could supply sediment to the lake, but erosion
327 appears inactive. The bedrock is too steep to retain soil beyond that required to support the trees. Sand
328 from the large deposit to the east is being reworked into the lake and thus the 53 cm deep B horizon of

329 this unit could be transported into the basin. This is consistent with sand sized particles in the lake
330 sediments (Fig. EA6).
331 Debar Pond (Fig. 2b) lies in a through valley between two higher hills. The mapped soil units are
332 diverse in nature. Thick organic accumulations, in the form of bogs and/or swamps, with more than 167
333 cm depth of material cover 3.2% of the basin. The remaining 96.8 % of the basin are soils derived from
334 tills of various types on moderate slopes with rocky or bouldery materials. Generally, these soils
335 transition from tills at lower elevation to more rocky texture at higher elevations. Slopewash may provide
336 a mechanism to transport old sediments and plant wax *n*-alkanes to lake basin. However, it would be
337 restricted to the area on the northeast side of the basin. Overland flow could not remove the organic
338 accumulation in the wetlands, and it may be trapped before entering the lake in this very low relief zone.
339 Wolf Pond (Fig. 2c) lies north-south in a broad valley. The non-bedrock parts of the drainage
340 basin have soils derived from lodgment tills, similar to Heart Lake. These are compact at depth and are
341 well-drained and do not promote runoff. The only source of organic matter is the upper 5 cm of the O soil
342 horizon and the B soil horizon. The delta indicates transport of some sediment. Any contribution from the
343 steep slopes and gullies is difficult to judge as they are likely still active. However, cuts are deeper than
344 the B horizon and thus are removing material from below any organic source. The ability of the soils to
345 drain reduces the potential for sheet wash.
346 Moose Pond (Fig. 2d) has a considerably larger drainage basin size (17.7 km^2) and basin relief
347 (692 m) than the other lakes. In the middle of this drainage basin, there is a broad flat infilled area with
348 organic material, and a small open water portion called Grass Pond. Moose Pond's large drainage basin is
349 covered with bedrock and lodgment till with a varying degree of slopes. The lodgment till is well drained
350 but has medium to high runoff potential. Quantifying any transport of older organic materials is
351 challenging because Grass Pond could serve as a trap for any material from a significant portion of the
352 basin and the evidence indicates former changes in water level. However, the lower stretches of the
353 stream draining the pond indicate reworking of alluvium which likely contained organic materials.

354 The subbottom profile (Fig. EA2) indicates little or no sediment accumulation on the slope and
355 thicker accumulation in the depressions with the thickest in the deepest basin. The geometry indicates that
356 only in the deeper part of the basin are the oldest sediments present. In sum, this distribution of sediment
357 indicates a focusing of the sediment as has been well documented in small lakes (e.g., Davis and Ford,
358 1982; Hilton et al., 1986; Blais and Kalff, 1995).
359 East Pine Pond (Fig. 2e) lies completely within drift deposited in the ice-contact environment.
360 The high ridge bordering the west and south shore is a portion of a small esker. The irregular and varying
361 depth depressions are characteristic of kettle topography. The water level is that of the regional ground
362 water table with adjacent streams and several lakes all at the same elevation. Given the stratified nature of
363 the parent material, the soils here are different than the other drainage basins. They are able to absorb any
364 rainfall and limit runoff. The steep slopes directly adjacent to the lake were observed to supply plant and
365 leaf materials directly into the lake. The irregular topography elsewhere keeps any organic accumulation
366 localized.
367 In sum, the deltas in Debar Pond, Moose Pond, and Wolf Pond indicate that sediment, and
368 potentially old sediment with *n*-alkanes, is being transported to the lake. The stream response to lake level
369 changes is likely the best candidate for older material to be delivered to each lake. Extensive areas of
370 these basins and the Heart Lake drainage basin have steep slopes with thin soils and localized erosion.
371 The topography around East Pine Pond permits modern materials to be transported into the lake, but the
372 well-drained soils will not permit transport of particulate materials to the lake via groundwater, and thus
373 cannot be large sources of old *n*-alkanes.
374
375 **3.2. Sediment age models**
376
377 Age models for each lake are shown in Figure 3 and EA4. For the two lake sites for which only
378 Bolivia cores were recovered, Debar Pond and Wolf Pond, maximum ages are 330 cal yr BP at 131.5 cm
379 and 1,210 cal yr BP at 142.5 cm, respectively. Overall, the sedimentation rate at Wolf Pond is half as fast

throughout the sampled sediment core, driven predominately by the young ^{14}C age at Debar Pond (330 ^{14}C yr BP), as compared to the two older samples at Wolf Pond (1,270 and 1,090 ^{14}C yr BP). ^{210}Pb sedimentation rates are similar at both lakes (Fig. EA5). For Debar Pond, sedimentation increases consistently through the record from about 12 mg m^{-2} y^{-1} for the 19th century to a contemporary rate of 30 mg m^{-2} y^{-1}. For Wolf Pond, sedimentation appears to show a background rate of ca. 10 mg m^{-2} y^{-1} from 1800-1850, although uncertainties are large. Sedimentation drops from 1880 to 1916 and remains relatively constant from 1950 to 2000 at ca. 18 mg m^{-2} y^{-1}, before rising to 30 mg m^{-2} y^{-1}.

The Heart Lake, East Pine Pond and Moose Pond age models integrate ^{210}Pb and radiocarbon samples from a combination of Bolivia and Livingston sediment cores (Fig. 3, EA3, and EA4; Table 2 and Data Table 1). Maximum ages as produced by the age-depth models are 7,800 cal yr BP at East Pine Pond (585.5 cm), 12,000 cal yr BP at Heart Lake (669.5 cm), and 13,400 cal yr BP at Moose Pond (693.5 cm). These dates provide minimum ages for the start of sedimentation at each lake, but actual lake basin initiation will likely predate these constraints. Overall, the sedimentation rate is similar throughout the three lake sites, averaging 0.1 cm y^{-1} (Fig. EA5). However, at Moose Pond this rate appears to increase at the very base of the sediment core, which is composed of glacially derived silts and sands. Conversely, through a similar interval at Heart Lake, the sedimentation rate slows (Schartman et al., 2020). No samples appropriate for radiocarbon dating were available from the comparable basal unit at the East Pine Pond sediment core and thus the sedimentation rate throughout the initial stages of lake basin inception is unknown. For Moose Pond, sedimentation rates show a uniform background rate of ca. 14 mg cm^{-2} y^{-1}, with a sharp increase beginning around the turn of the 20th century to a contemporary rate of 30 mg cm^{-2} y^{-1}. For East Pine Pond, sedimentation rates show what appears to be a 19th century background of ca. 8 mg cm^{-2} y^{-1}, before rising around 1920 to peak in 1955 at 30 mg cm^{-2} y^{-1}. At Heart Lake, rates are generally faster, as sedimentation increases approximately linearly from about 20 mg m^{-2} y^{-1} at the turn of the 19th century to a contemporary rate of ca. 70 mg m^{-2} y^{-1} (Fig. EA5).

Finally, we note that the two radiocarbon samples from Wolf Pond have similar age-depth relationships as those from the surface sediment cores at East Pine and Moose Ponds. At East Pine Pond,

406 a sample collected at 110.25 cm of depth was dated to 1,400 ^{14}C yr BP, while at Moose Pond a sample
407 from 121.25 cm of depth was dated to 1,500 ^{14}C yr BP. Conversely, Debar Pond surface sediment
408 radiocarbon results appear more similar to Heart Lake's, which has an age of 675 ^{14}C yr BP for a sample
409 collected from 145 cm of depth. In short, age-depth relationships from all five lake sites are largely
410 similar, and from the input ages and resultant age models, we see no evidence for distinct outliers among
411 sedimentation into each lake. Based on sedimentation rate and CSRA sample thickness, the overall mean
412 and median time integrated in each CSRA sample is 69 and 38 yr, respectively (Table EA2).
413
414 **3.3. *n*-Alkane ^{14}C analyses**
415
416 Samples in all Bolivia surface cores from which the CSRA samples were collected had mean
417 sedimentation ages that ranged from 40 to 1,385 cal yrs BP. The *n*-alkane $\Delta^{14}C_{initial}$ values for these
418 samples ranged from –6.4 to –276.7‰, corresponding to sediment ^{14}C ages between 470 and 3,950 yr BP.
419 The *n*-alkane $^{14}C\ age_{initial}$, the ^{14}C age of the *n*-alkanes at the time of sediment deposition, ranged from –
420 105 ± 86 to 2,440 ± 94 ^{14}C yr (Fig. 4 and 5). The mean *n*-alkane $^{14}C\ age_{initial}$ is 630 ± 560 ^{14}C yr (1σ, n =
421 15), which includes one sample (2-MB) at Moose Pond ($^{14}C\ age_{initial}$ of 2,440 ^{14}C yr) that is substantially
422 older than the rest of the samples (~5x the median $^{14}C\ age_{initial}$ of 490 ^{14}C yr). Moose Pond had distinctly
423 higher contributions of sand sized particles (Fig. EA6) consistent with alluvial sediment transport, and the
424 Moose Pond core location was located near a delta downstream of a wetland complex on the eastern side
425 of the drainage basin (Fig. 2). Given these factors, we speculate that sample 2-MB was deposited during a
426 storm event (see Section 4.1), and remove it from further analyses, unless otherwise noted. When sample
427 2-MB is removed, the mean initial *n*-alkane age drops to 500 ± 250 ^{14}C yr (1σ, n = 14). There is no
428 statistical difference in the *n*-alkane $^{14}C\ age_{initial}$ between these five lakes (p = 0.1; ANOVA), although we
429 note the sample size is small.

Samples in the longer Livingstone cores from East Pine, Debar, and Moose Ponds from which the CSRA samples were collected had sedimentation ages that ranged from 3,120 to 13,140 cal yr BP. These samples had *n*-alkane $\Delta^{14}C_{initial}$ values that ranged from 178.4 to –53.3‰ and correspond to sediment ^{14}C ages between 3,470 and 11,450 yr BP. The *n*-alkane ^{14}C $age_{initial}$ ranged from –25 ± 239 to 520 ± 118 ^{14}C yr (Fig. 4 and 5) with a mean of 250 ± 160 ^{14}C yr (1σ, n = 9). There is no statistical difference in the *n*-alkane ^{14}C $age_{initial}$ for these older sediments from the three lakes ($p = 0.1$; ANOVA), although we note again the small sample size.

Among all samples collected from the 5 lakes, the mean *n*-alkane ^{14}C $age_{initial}$ was 400 ± 255 ^{14}C yr (1σ, n = 23). We explored the *n*-alkane ^{14}C $age_{initial}$ values among all lakes to determine if any of the lakes differed significantly from each other, but we found no evidence of this ($p = 0.4$; ANOVA). To explore if there were any differences in *n*-alkane ^{14}C $age_{initial}$ values with sediment deposition age (Fig. 5), we compared recent to older sediment by assigning samples to bins with sediment ages younger and older than 1, 3 and 6 cal kyr BP. For sediment ages older than 1 cal kyr BP, the mean *n*-alkane ^{14}C $age_{initial}$ is 220 ± 195 ^{14}C yr (1σ, n = 11) and for younger than 1 cal kyr BP, the mean is 565 ± 180 ^{14}C yr (1σ, n = 12). This difference of 345 ^{14}C yr is significant (t-test, $p = 0.0003$). These results are also similar using 3 and 6 cal kyr BP cutoffs. At the individual lake level, the total sample size is small preventing a statistical test, but qualitatively this pattern is true (means are smaller for the >1 cal kyr BP sediments). Combined there is a statistically significant decrease in *n*-alkane ^{14}C $age_{initial}$ values with increasing sediment age, although the relationship has low explanatory power in a least squares regression ($R^2 = 0.26$, n = 23 $p = 0.01$; sediment age natural log transformed for normality).

For comparison with other studies, we also measured MTT_{wax}. The mean MTT_{wax} for all samples (excluding the outlier at Moose Pond) was 390 ± 240 cal yr BP (1σ, n = 23; Table EA2). MTT_{wax} values were highly correlated with initial *n*-alkane ages (linear least squares regression; $R^2 = 0.86$, $p < 0.0001$), but are offset in age due to differences between ^{14}C yrs and calibrated years. Similar to the comparisons

454 above, we found no difference in MTT_{wax} among lakes. MTT_{wax} also increases from old to young
455 sediment ages, similarly to *n*-alkane ^{14}C $age_{initial}$.
456 The *n*-alkane accumulation rate (MAR_{wax}) was measured using the sediment rate, sediment
457 density, and *n*-alkane concentrations (Table EA2). Debar Pond had the highest mean accumulation rate
458 (0.45 µg cm^{-2} yr^{-1}; ANOVA $p = 0.001$; Tukey HSD). The other lakes were not statistically different from
459 one another. MAR_{wax} is not correlated with lake or catchment area. *n*-Alkane ^{14}C $age_{initial}$ and MTT_{wax} was
460 also not correlated with the *n*-alkane accumulation rate (MAR_{wax}) either for all samples, or by lake.
461
462 **4. DISCUSSION**
463
464 **4.1 *n*-Alkane ^{14}C ages**
465
466 For the five Adirondack lakes, we found *n*-alkane ^{14}C $age_{initial}$ values were similar among the
467 lakes (400 ± 255 ^{14}C yr; Fig. 4 and 5). This is despite differences in the drainage basin and lake size, basin
468 relief, basin geomorphology, soil thickness and potential to store and transport old sediments and *n*-
469 alkanes to the lake sediments. The contribution of older *n*-alkanes increases through time with greater
470 offsets in sediments deposited within the last 1 kyr (Fig. 5). Below, we compare these results to those
471 observed in other studies.
472 For comparison to other studies, we also report MTT_{wax} ages (e.g., Douglas et al., 2018). These
473 values are similar in magnitude to our *n*-alkane ^{14}C $age_{initial}$ values (Table EA2) and therefore can be
474 directly compared to values reported in other studies. Our age offsets are small compared to other studies
475 of Holocene sediments from contrasting depositional settings. These include karstic tropical lakes
476 (Douglas et al., 2018), a glacial lake in Switzerland (Gierga et al., 2016), a varved coastal fjord
477 (Smittenberg et al., 2006), and the Congo River Fan (Schefuß et al., 2016) which all had much larger age
478 offsets with a maximum of 8,000 cal yr (Smittenberg et al., 2006). The Adirondack MTT_{wax} values are
479 similar in magnitude to those observed at Lake Sopensee in Switzerland during the early to mid-Holocene

480 (Gierga et al., 2016). In contrast, from ~3 kyr to present, anthropogenic land clearing at Lake Sopensee
481 increased the MTT_{wax} to millennial-scale values (~1-8 kyr), whereas MTT_{wax} in the Adirondack lakes
482 remained around 250 years. The MTT_{wax} of Central American lakes also varied over the Holocene due to
483 anthropogenic land use change such as deforestation or agricultural cultivation that decreased the
484 apparent terrestrial residence times of *n*-alkanes prior to deposition in lakes (Douglas et al., 2018).
485 The earliest known Paleo-Indian sites in the region date to 9,000 BCE. During the pre-colonial
486 period, Iroquoian and Algonquin peoples used the Adirondacks seasonally for fishing, hunting and
487 trapping, but did not permanently settle or farm extensively in the area possibly due to the mountainous
488 terrain and acidic soil, particularly in the High Peaks (Otis, 2018). Given the lack of evidence for a major
489 change in the longstanding Indigenous presence and seasonal hunting practices in the Adirondacks at
490 around 1,000 yr BP, we doubt that Indigenous land use is related to the apparent increase in age offsets at
491 that time. We also do not expect that vegetation shifts had a large effect on the observed increase in *n*-
492 alkane initial age after 1,000 cal yr BP because the existing Adirondack vegetation zones were established
493 within the past 2,000 years and remain largely stable to the modern (Whitehead and Jackson, 1990;
494 Schartman et al., 2020). The observed increase in *n*-alkane age offsets does align with regional Medieval
495 Climate Anomaly evidence in sedimentary charcoal and *Pinus* pollen records from Wolf Lake in the
496 Adirondacks (Stager et al., 2016) and from Southern New York State (Pederson et al., 2005) suggesting
497 increased watershed erosion during drought and fire conditions, at ~1,000 ^{14}C yr BP and from ~800–1300
498 A.D., respectively. This is consistent with tree-ring based model reconstructions of Mississippi Valley
499 Droughts and Stine megadroughts in North America during the last millennium, with arid conditions
500 extending into the Adirondacks from 940-985 AD and 832-1074 AD, respectively (Cook et al., 2010;
501 Menking et al., 2012). We therefore speculate that episodic, event-based climatic changes are linked to
502 the apparent increase in *n*-alkane age offsets through time, rather than anthropogenic disturbance or basin
503 properties, particularly because this trend was observed across all basins (Fig. 5B).
504 The largest anthropogenic disturbance in the Adirondacks began in the early 1800s with the first
505 sawmills established near the lakes studied here between 1804 and 1810. However, logging in this region

506 was selective within individual areas and focused on specific species rather than deforestation. In contrast,
507 agricultural land use in the region did involve clearcutting, but not in the basins studied here. Logging
508 reached a peak by 1865 with specific species (i.e., white pine, spruce) timber supplies exhausted by 1885
509 (Fox, 1902; Defebaugh, 1906; McMartin, 1994). Between 1870-1880, sedimentation rates are higher in 4
510 (Debar Pond, East Pine Pond, Moose Pond, and Wolf Lake) out of the 5 lakes. Sediment fluxes increased
511 ~1.5 to 2x background levels at these 4 lakes, indicating that logging may have increased the inputs of
512 soil-derived plant wax into the lakes during this time. Although we have limited *n*-alkane CSRA data for
513 this time, MAR_{wax} is higher in these four lakes for the most recent samples that correspond to around this
514 same time. However, $^{14}C\ age_{initial}$ values are no different for this time period (Fig. 5) despite increased
515 sediment and *n*-alkane flux. This could be due to insufficiently large or prolonged change in
516 sedimentation rate over this period to affect observed *n*-alkane age offsets, or because the CSRA sample
517 coverage, or time averaging, over the sampled interval of sediment lacked sufficient resolution. The
518 largest apparent initial *n*-alkane age observed in our study (2,440 ^{14}C yr) was recorded at Moose Pond
519 (Table EA2). Moose Pond has the largest lake and catchment areas as well as the largest catchment relief
520 of the sites studied here. Age offsets in the other samples from this lake were not consistently or
521 significantly higher than at any other lake, suggesting that this one sample may have a large age offset
522 due to a transient factor, such as a storm event. This basin is the most complex of the lakes studied (Fig.
523 2), the eastern side of the drainage basin contains stream and wetland environments and has the greatest
524 reservoir of soils in the drainage basin. Our core location is nearby the delta downstream of this complex
525 terrain and therefore, it is conceivable that a storm may have eroded and transported older sediments and
526 thus much older *n*-alkanes. Of the sites studied here, this lake has the highest amount of sand sized
527 particles supporting an alluvial sediment source (Fig. EA6).
528
529 **4.2 Mechanisms for *n*-alkane age offsets**
530
531 In this study and others, terrestrial plant waxes almost always have some degree of age offset

relative to sediments, indicating terrestrial storage or residence time prior to incorporation into sediments. In general, the age of terrestrial plant wax in sediments represents a mix of waxes that are penecontemporaneous with sedimentation (e.g., aerosols, litterfall) and either 1) older, reworked waxes from the sediment or soils in the catchment and/or 2) reworked petrogenic compounds. In this study, petrogenic sources of *n*-alkanes can be ruled out as a source because the metamorphic bedrock in the Adirondacks is free of plant wax *n*-alkanes, as mentioned above. Lakes in the Adirondacks therefore receive *n*-alkanes from penecontemporaneous age sources and older sources of *n*-alkanes stored on the landscape.

Penecontemporaneous inputs of *n*-alkanes include aerosols and airborne litterfall (Section 1). Wet-deposition of aerosol *n*-alkanes have been estimated to contribute to 15% of the flux to lake sediments in temperate North America (Meyers and Kites, 1982). This is consistent with observations from Europe that atmospheric deposition rates of *n*-alkanes over land account for ~20% of accumulation rates in lake sediments (Nelson et al., 2018). Atmospheric deposition was also estimated to be as high as ~50% of the annual input of *n*-alkanes in temperate North American lakes (Doskey, 2000). These differences in aerosol contributions vary among studies and may be dependent on many factors including *n*-alkane source area, seasonality, atmospheric conditions affecting dry- and wet-deposition and precipitation totals. Aerosol *n*-alkanes therefore potentially contribute to an annual duration pool of *n*-alkane inputs to Adirondack lakes.

Airborne litterfall is also an important source for sedimentary *n*-alkanes in the Adirondacks and other forested drainage basins, with approximately seasonal to annual-scale temporal integration. Most of the lake catchments in this study were dominated by deciduous angiosperm forests or mixed deciduous angiosperm and conifer forests (Freimuth et al., 2020), and would be consistent with pulses of litterfall during autumn. During the October 2016 field campaign in the Adirondacks, we observed direct litterfall into the lake, recently fallen leaves accumulating on lake shores, and leaves suspended in the water column (Fig. EA7). Additionally, broadleaf and needleleaf material was occasionally observed in the sediment cores. Estimates of annual transport of airborne litterfall in temperate North American lakes is

558 typically 320-350 (and up to 500) gC m^{-1} of shoreline (Jordan and Likens, 1975; Gasith and Hosier,
559 1976). The relative contribution of airborne leaf litter to total organic matter flux generally decreases
560 exponentially with increasing lake area and distance from the shoreline (Gasith and Hosier, 1976). This
561 latter fact is also supported by leaf taphonomy studies (e.g., Spicer and Wolfe, 1987; Greenwood, 1991).
562 In the Adirondacks, we would therefore expect litterfall (and therefore penecontemporaneous *n*-alkane
563 inputs) to contribute less to sediments at Moose Pond than at other lakes with smaller areas (Table 1).
564 However, this is not supported by MAR_{wax}, as Moose Pond, the largest of the lakes, is not significantly
565 different from East Pine Pond, Heart Lake, and Wolf Pond.

566 The lakes in this study were selected to capture a range of drainage basin morphologies (Fig. 2;
567 Table 1), and thereby a range of potential *n*-alkane storage and erosion processes from catchment soils.
568 The deltas in Debar, Moose, and Wolf Ponds support sediment transport directly into the lake and would
569 suggest that sediments, soils, and thus *n*-alkanes are eroded from areas upstream within the catchment and
570 transported into the lakes. These areas are likely candidates for old *n*-alkanes and could result in the
571 observed age offsets. Changes in lake level would be the best mechanism to activate erosion within these
572 drainage basins for delivery of old *n*-alkanes to lake sediments. In contrast, extensive areas of these
573 drainage basins (e.g., Heart Lake) are steeply sloped with thin soils and have very localized erosion. Due
574 to the erosion style and lack of old soils, these steep sloped areas cannot be a source of old (1000 yrs) *n*-
575 alkanes. East Pine Pond's topography is unique compared to the other drainage basins as it is
576 characterized by relatively low relief. The catchment does have sufficient slopes for modern materials to
577 be transported into the lake, but the surrounding well-drained soils cannot be large sources of old *n*-
578 alkanes as there is no evidence for deep soil erosion.

579 *n*-Alkane ^{14}C age offsets appear to increase through time with the largest age offsets in the past 1
580 kyr. However, even in the oldest sediments, and sediments predating land disturbance by European
581 settlement, an age offset is apparent (Fig. 5). This age offset exists in the oldest samples studied from the
582 Livingstone cores at East Pine Pond, Heart Lake, and Moose Pond. This observation that age offsets exist
583 not long after drainage basin formation is informative as it suggests that *n*-alkane age offsets can occur

584 without deep soil erosion and do not necessitate a source of significantly older *n*-alkanes (1000 yrs).

585 In the Adirondack lakes studied here, *n*-alkane ^{14}C age offsets will be controlled by mixing
586 between penecontemporaneous sources of *n*-alkanes and older reworked soil-derived *n*-alkanes from the
587 catchment. The challenge is differentiating mixing of small amounts of relatively old (~10,000 yr) soil-
588 derived *n*-alkanes from large amounts of relatively recent (~250 yr) soil derived *n*-alkanes. Figure 6
589 illustrates this point with a mixing model that incorporates the fraction of reworked old *n*-alkanes of
590 differing ^{14}C ages resulting in a range of *n*-alkane ^{14}C $age_{initial}$ values. This example uses a sediment age of
591 1,000 cal yr BP and is a good approximation for the range of sediment ages measured in this study and for
592 many studies that focus on Holocene aged sediments. For comparison, a histogram of the measured *n*-
593 alkane ^{14}C $age_{initial}$ values is plotted, and the dashed line represents the median *n*-alkane ^{14}C $age_{initial}$ of 440
594 ^{14}C yr. This median *n*-alkane ^{14}C $age_{initial}$ value could be explained by mixing of a minimum fraction
595 (~0.05) of old-aged *n*-alkanes (15,000 ^{14}C yr; 14,000 yr age offset) or up to a much larger fraction (~0.9)
596 of young-aged *n*-alkanes (1,500 ^{14}C yr; 500 yr age offset). This model is an oversimplification as
597 reworked *n*-alkanes likely represent a distribution of ages and these ages likely evolve through time as the
598 drainage basin develops. Nonetheless, it is informative for thinking about the *n*-alkane age offsets and
599 places some constraints on the endmembers of young and old aged *n*-alkanes and their fractions.

600 As discussed above, the geomorphology of these drainage basins does not support extensive
601 erosion of old soil-derived *n*-alkanes at each of the lakes as the majority of these drainage basins lack the
602 reservoirs, thick soils and sediments of old age, and lack the mechanisms for erosion and deep incision.
603 Each of the lakes studied here have similar age offsets, despite differences in basin morphology, and these
604 age offsets are largely maintained through time. Combined, this strongly suggests the observed *n*-alkane
605 ^{14}C age offsets are caused by incorporation of large amounts of *n*-alkanes with relatively recent ages ($\leq$
606 1000 ^{14}C yrs). A detailed study of the *n*-alkanes ages in the soil profiles from each of the lake basins was
607 outside the scope of this study. Despite being hydrophobic and having incredibly low solubility in water,
608 *n*-alkanes and other lipids have been found in water-soluble fractions of surface soils, most likely due to
609 colloidal dispersion (Nierop and Buurman, 1998), a mechanism that may facilitate sub-surface transport

of aged lipids from deep soil horizons to lake sediments in karst geology (Douglas et al., 2014). It is unclear whether the same process is feasible in the glacial geology of the Adirondacks, but it cannot be directly assessed based on the data generated in this study. We note, however, that Nierop and Buurman (1998) found that the water-soluble organic matter produced from surface soils comprised only ~0.01% of the total soil and, if present in the Adirondacks, may therefore be a minor component of the total terrestrial plant-derived lipids exported to lake sediments, when compared with the potential flux from eroded soils and leaves.

Soil *n*-alkanes are thought to belong to a passive pool of carbon characterized by slow turnover times(Huang et al., 1996; Huang et al., 1999; van der Voort et al., 2017), likely due to selective preservation through mineral interactions or associations with stable organic matter fractionations (Lichtfouse et al., 1998a; Lichtfouse et al., 1998b). We note that mineral-bound, aged plant waxes from B-horizon soils can be preferentially preserved and settled out of the lake water column due to mineral association, and therefore selectively preserved relative to more labile, rapidly degraded waxes from A-horizon soils (Vonk et al., 2010). It may therefore be possible to store, age, and supply old (100s to ~1000 ^{14}C yrs) *n*-alkanes from the uppermost surface soils in the lake catchments, and we cannot rule out some supply or selective preservation of deeper soils with much older *n*-alkane ages, as discussed above for some lakes (i.e. Moose Pond), but we argue this process is minor given the striking similarities among the lakes. With the current data, it is not possible to find a single solution to the mixing problem described above, but we suspect that the fraction of reworked *n*-alkanes with age offsets $\leq$ 1000 ^{14}C yrs is large. Mixing of *n*-alkanes of multiple ages has important implications for the attenuation of climate signals embedded in their carbon and hydrogen isotopic compositions. Below, we discuss the implications of the *n*-alkane mixing for paleoclimate reconstructions.

4.3 Implications for paleoclimate reconstruction

Lake sediments can provide paleoclimate records at high temporal resolution, and several studies

636 have made use of this to characterize climatic and ecological change using sedimentary plant wax at
637 centennial to sub-decadal scales (Feakins et al., 2014; Rach et al., 2014). Prolonged storage of *n*-alkanes
638 (but also other plant wax compounds) in soils prior to deposition in lake sediments can compromise the
639 fidelity of plant wax *n*-alkanes to record high-frequency changes in past climate or vegetation (e.g.,
640 French et al., 2018).

641 For paleo-applications, small lakes in forested drainage basins that have no history of
642 anthropogenic disturbances, such as deforestation or agricultural land use, and that have been
643 continuously forested, are thought to be influenced the least by *n*-alkane age offsets (e.g., Gierga et al.,
644 2016). In the case of the Adirondacks, where we expect that such anthropogenic land use disturbance was
645 minimal until the 1850s, centennial-scale *n*-alkane $^{14}C\ age_{initial}$ values are prevalent, with an overall mean
646 of 400 ± 255 ^{14}C yr (Fig. 5). This centennial-scale *n*-alkane ^{14}C age offset has the potential to reduce the
647 fidelity of sedimentary plant wax isotopes to past precipitation or vegetation changes. This distortion of
648 the proxy record can include two main effects: attenuation of the magnitude of a climate signal, and lags
649 relative to the temporal structure of the climate signal. Proxy attenuation and lags are not mutually
650 exclusive and the dominance of one or the other is a function of the fractional abundance and age
651 distribution of both fast- and slow-cycling pools of plant wax that contribute to lake sediments (Douglas
652 et al., 2014; French et al., 2018). For lags to dominate over attenuation would require very high fractional
653 abundance (~0.95) of slow-cycling (~millennial) wax with a relatively small age structure standard
654 deviation (Douglas et al., 2014). In the Adirondacks, our mixing model (Fig. 6) suggests that to reach the
655 mean age offset of ~400 yr with a slow-cycling wax pool of millennial age would require a fractional
656 contribution to the total sedimentary plant wax of between ~0.1 to ~0.4 at most. This suggests that the
657 Adirondack sedimentary plant wax records are more likely to reflect attenuation than significant lags,
658 consistent with the relatively high-frequency (centennial-scale), high-amplitude (20-30‰) deglacial plant
659 wax δ^2H shifts in Adirondack lake records (Schartman et al., 2020). The exact degree of attenuation is
660 complex and will depend not only on the age structure of sedimentary plant wax but also on the isotopic
661 composition of these old *n*-alkanes, and the magnitude of isotopic change associated with the

precipitation or vegetation event recorded in plant wax isotopes.

We caution that this does not imply that the isotopic signal recorded in *n*-alkanes is not useful, or that centennial-scale pre-aging is to be expected in all lake sediments; indeed, *n*-alkane molecular distribution and $\delta^{13}C$ data from some lakes suggests rapid (even sub-decadal) transfer of long-chain *n*-alkanes into sediments (Lane et al., 2016; Aichner et al., 2018). Results from this study do, however, indicate that sedimentary long-chain *n*-alkanes have some degree of time averaging or attenuation, which is important to account for when trying to assess the magnitude and timing of isotopic proxies for paleoclimate applications, especially across high-frequency events. In the case of the Adirondacks, precipitation $\delta^{2}H$ records generated from lake sediment *n*-alkanes for the Late Glacial through the Holocene are likely attenuated over a few hundred years and therefore decadal to centennial-scale isotopic signals may not be recorded, but centennial to millennial scale changes would be captured (Schartman et al., 2020).

In summary, *n*-alkane ^{14}C age offsets are important, but for forested temperate lake catchments, similar to these Adirondack lakes, the age offsets are much smaller than those observed for lakes that may have anthropogenic disturbances. With proper site selection, it is possible to minimize these *n*-alkane age offsets. This can be accomplished by selecting lakes in drainage basins that lack petrogenic plant wax sources, that have minimal soil storage potential, and that lack relief and fluvial input to minimize soil erosion. Avoiding sites with anthropogenic soil disturbance is key, if the focus is on paleoclimate and not on human activities. Additionally, modeling experiments could be used to explore possible signal attenuation, informed by possible *n*-alkane age offsets and isotopic compositions of old *n*-alkanes, to estimate signal to noise and signal attenuation.

5. CONCLUSIONS

Plant wax *n*-alkane ages were compared to sediment ages (based on ^{210}Pb and terrestrial

687 macrofossil ^{14}C chronologies) from five Adirondack lakes across a range of lake and catchment sizes and
688 morphologies. A primary objective of this study was to test whether terrestrially derived long-chain *n*-
689 alkane sediment age offsets are dependent on factors inherent to a drainage basin (e.g., size,
690 geomorphology, soil reservoirs) or whether they respond to transient factors that vary through time. Age
691 offsets for *n*-alkanes relative to sediments ranged from penecontemporaneous to 2,440 ^{14}C yr with a mean
692 *n*-alkane ^{14}C $age_{initial}$ of 400 ± 255 ^{14}C yr. We found no systematic relationship between sediment *n*-alkane
693 age offsets and the drainage basin characteristics represented within the five study lakes, suggesting either
694 insufficient geomorphic variation among the sampled sites, or that the primary controls are transient
695 factors (e.g., climate/lake level change or episodic land use/cover change) rather than basin-specific
696 properties. In these lakes, *n*-alkane age offsets increase from a mean of 220 ± 195 ^{14}C yr (1σ, n = 11)
697 between 1 and 13 cal kyr BP to 565 ± 180 ^{14}C yr (1σ, n = 12) within the last 1 kyr, possibly reflecting
698 drying associated with regional expression of the Medieval Climate Anomaly. Based on our original
699 hypothesis and trends observed in prior studies, we expected that as soil reservoirs developed over the
700 Holocene, the age offsets would become substantially larger (millennial-scale) than we observed (a ~340
701 yr increase). In these Adirondack lakes, the extent to which long-stored soil-derived *n*-alkanes could be
702 eroded from the drainage basin is limited, as the majority of these drainage basins lack the reservoirs
703 (thick soils of old age) and likewise lack the mechanisms for erosion of and deep incision into soils and
704 sediments. Given that the *n*-alkane age offsets are established early after basin formation and
705 sedimentation, before any appreciable soils could have developed, it is conceivable that the lake sediment
706 *n*-alkane age offsets are caused by incorporation of large amounts of *n*-alkanes that are likely ≤ 1000 ^{14}C
707 yrs older than the age of sedimentation. Testing this would require detailed CSRA studies of catchment
708 soils in many locations within contrasting catchments.

709 Regardless of the exact mechanisms, climatic and vegetation signals recorded in the isotopic
710 composition of *n*-alkanes will reflect this mixing of older *n*-alkanes, and this will contribute to signal
711 attenuation. This does not suggest that important information cannot be extracted from the isotopic

composition of *n*-alkanes, but it does suggest that the resolution may be limited by the extent of the *n*-alkane age-offset and the complexities of mixing of multiple sources with different ages and isotopic compositions. For lakes in the Adirondacks, *n*-alkanes are attenuated on a centennial timescale and subcentennial resolution records are not possible. Being aware of those limitations is key (e.g., Schartman et al., 2020). Future studies should consider the drainage basin geomorphology and potential for storage and erosion of old *n*-alkanes in the site selection process.

FIGURE CAPTIONS:

Figure 1. Geographic location and topography of the Adirondack Park (ADK) and study lakes.

Figure 2. Topographic maps of the study sites depicting lake catchment extent, lake area and coring locations for Heart Lake (A), Debar Pond (B), Wolf Pond (C), Moose Pond (D) and East Pine Pond (E). Catchment topography is shown as shaded relief and catchment borders are indicated by the light blue line. Outside the catchment, elevation contours are depicted with red lines. The contour interval is 5 m except at Moose Pond and Debar Pond where it is 10 m. Coring locations are indicated by white circles on all lakes. Scale varies between catchment maps.

Figure 3. Bayesian age-depth models constructed for the study lakes using Bacon v2.2 (Blaauw and Christen, 2011). Sediment depth (cm) is plotted against age (cal yr BP) with variable scales. The solid red line is the weighted mean solution of all the Monte Carlo iterations with darker shading indicating the increased likelihood that the model produces iterations that pass through that section. Dashed black lines demarcate the 95% confidence interval of each model. Model inputs, radiocarbon and ^{210}Pb age distributions, model stability, prior and posterior accumulation rate and memory, as generated by Bacon

737 v2.2, are presented in Figure EA4. Blue symbols indicate depths at which CSRA samples were taken
738 from Bolivia cores (squares) and Livingstone cores (circles).
739
740 **Figure 4.** Boxplots indicating the A) *n*-alkane $\Delta\Delta^{14}C_{initial}$ values and the B) *n*-alkane ^{14}C $age_{initial}$ values for
741 each lake with the median, upper and lower quartiles, and maximum and minimum values indicated.
742 Circles indicate outliers. Median values are shown for reference. Total number (n) of samples is indicated.
743
744 **Figure 5.** *n*-Alkane ^{14}C $age_{initial}$ (^{14}C yr) by sediment age (cal yr BP) for each of the five lakes. Sediment
745 age is plotted on A) linear and B) logarithmic scales. The sediment age error bars (1σ) are the reported
746 uncertainties from Bacon sediment age model. The ^{14}C $age_{initial}$ error bars are the propagated uncertainties
747 in the $\Delta^{14}C_{initial}$ values, which includes the error in the blank corrected Fm (1σ), the uncertainty in the
748 sediment age (t), and the uncertainties reported for $\Delta^{14}C_{atm}$ (Reimer et al., 2013). Error propagation was
749 determined using the Monte Carlo method of error propagation.
750
751 **Figure 6.** A) An isotopic mixing model of *n*-alkane ^{14}C $age_{initial}$ values as a function of the fraction of
752 reworked *n*-alkanes with varying ages. Sediment age for all scenarios is 1,000 ^{14}C yr BP and is
753 representative for the range in lake sediment ages reported in this study (e.g., Holocene to Late Glacial).
754 B) A probability histogram of *n*-alkane ^{14}C $age_{initial}$ values from all study lakes. For comparison, the
755 probability density is shaded for comparison to (A). The dashed line represents the measured median *n*-
756 alkane ^{14}C $age_{initial}$ value of 440 ^{14}C yr from all Adirondack lakes. The dashed line provides an illustration
757 of the possible fractions of old reworked *n*-alkanes that could account for an age offset of 440 ^{14}C years
758 for a range of old *n*-alkane ages. Note, an old *n*-alkane age of 1,250 ^{14}C yr BP, for example, would be 250
759 ^{14}C yr older than the sediment at the time of deposition.
760
761

RESEARCH DATA

Research data is provided in Data Table 1 and Data Table 2.

Data Table 1. ^{210}Pb and ^{137}Cs data, age models, and sedimentation rates for the recent sediments.

Data Table 2. *n*-Alkane sample information for compound specific radiocarbon analysis (CSRA).

ACKNOWLEDGMENTS

We thank Sarah Feakins, Peter Douglas, and two anonymous reviewers for their helpful comments that improved this manuscript. We thank Li Xu, Mary Lardie, and Ann McNichol at the National Ocean Sciences Acceleratory Mass Spectrometry (NOSAMS) Sample Prep Lab for assistance with radiocarbon sample preparation. We also thank the New York State Department of Environmental Conservation for sampling permits (TRP #2349/10310), the Adirondack Mountain Club for access to Heart Lake, and the State University of New York College of Environmental Science and Forestry for access to Wolf Pond. Thanks to Helen Eifert and Elliot Boyd for field sampling assistance, to Kelly Grogan for laboratory assistance, and to Andrew Diefendorf for designing and building the core storage unit and core splitter. This research was supported by the US National Science Foundation (EAR-1229114 to AFD, EAR-1636740 to AFD and TVL, EAR-1636744 to AK Stewart, and OCE-1239667 to NOSAMS) and by a University of Cincinnati Research Council award and a University of Cincinnati Graduate Student Fellowship to EJF.

784 **REFERENCES:**

785

786 Aichner B., Ott F., Słowiński M., Noryśkiewicz A.M., Brauer A. and Sachse D. (2018) Leaf wax *n*-alkane
787 distributions record ecological changes during the Younger Dryas at Trzechowskie paleolake
788 (northern Poland) without temporal delay. *Clim. Past* **14**, 1607-1624.

789 Anderson G.M. (1976) Error propagation by the Monte Carlo method in geochemical calculations.
790 *Geochim. Cosmochim. Acta* **40**, 1533-1538.

791 Appleby P.G. and Oldfield F. (1978) The calculation of lead-210 dates assuming a constant rate of supply
792 of unsupported 210Pb to the sediment. *CATENA* **5**, 1-8.

793 Binford M.W. (1990) Calculation and uncertainty analysis of ^{210}Pb dates for PIRLA project lake sediment
794 cores. *J. Paleolimnol.* **3**, 253-267.

795 Blaauw M. and Christen J.A. (2011) Flexible paleoclimate age-depth models using an autoregressive
796 gamma process. *Bayesian Anal.* **6**, 457-474.

797 Blais J.M. and Kalff J. (1995) The influence of lake morphometry on sediment focusing. *Limnol.*
798 *Oceanog.* **40**, 582-588.

799 Bowen G.J., Nielson K.E. and Eglinton T.I. (2019) Multi-Substrate Radiocarbon Data Constrain Detrital
800 and Reservoir Effects in Holocene Sediments of the Great Salt Lake, Utah. *Radiocarbon* **61**, 905-
801 926.

802 Bray P.S., Brocks J.J. and George S.C. (2014) ^{14}C analysis of aliphatic hydrocarbon fractions from the
803 hypersaline Lake Tyrrell, southeast Australia. *Org. Geochem.* **73**, 29-34.

804 Carvalhais N., Forkel M., Khomik M., Bellarby J., Jung M., Migliavacca M., Mu M., Saatchi S., Santoro
805 M., Thurner M., Weber U., Ahrens B., Beer C., Cescatti A., Randerson J.T. and Reichstein M.
806 (2014) Global covariation of carbon turnover times with climate in terrestrial ecosystems. *Nature*
807 **514**, 213-217.

808 Casper S.J., Krey L. and Proft G. (1985) Fallen leaves in Lake Stechlin, in: Casper, S.J. (Ed.), Lake
809 Stechlin: A Temperate Oligotropihic Lake. Springer Netherlands, Dordrecht, pp. 401-409.

Conte M.H., Weber J.C., Carlson P.J. and Flanagan L.B. (2003) Molecular and carbon isotopic composition of leaf wax in vegetation and aerosols in a northern prairie ecosystem. *Oecologia* **135**, 67-77.

Cook E.R., Seager R., Heim Jr R.R., Vose R.S., Herweijer C. and Woodhouse C. (2010) Megadroughts in North America: placing IPCC projections of hydroclimatic change in a long-term palaeoclimate context. *Journal of Quaternary Science* **25**, 48-61.

Cranwell P.A., Eglinton G. and Robinson N. (1987) Lipids of aquatic organisms as potential contributors to lacustrine sediments—II. *Org. Geochem.* **11**, 513-527.

Davis M.B. and Ford M.S. (1982) Sediment focusing in Mirror Lake, New Hampshire. *Limnol. Oceanog.* **27**, 137-150.

Defebaugh J.E. (1906) *History of the lumber industry of America*. The American lumberman, Chicago.

Diefendorf A.F., Freeman K.H., Wing S.L. and Graham H.V. (2011) Production of *n*-alkyl lipids in living plants and implications for the geologic past. *Geochim. Cosmochim. Acta* **75**, 7472-7485.

Diefendorf A.F. and Freimuth E.J. (2017) Extracting the most from terrestrial plant-derived *n*-alkyl lipids and their carbon isotopes from the sedimentary record: A review. *Org. Geochem.* **103**, 1-21.

Doskey P.V. (2000) The air–water exchange of C15–C31 *n*-alkanes in a precipitation-dominated seepage lake. *Atmos. Environ.* **34**, 3981-3993.

Douglas P.M.J., Pagani M., Eglinton T.I., Brenner M., Curtis J.H., Breckenridge A. and Johnston K. (2018) A long-term decrease in the persistence of soil carbon caused by ancient Maya land use. *Nat. Geosci.* **11**, 645-649.

Douglas P.M.J., Pagani M., Eglinton T.I., Brenner M., Hodell D.A., Curtis J.H., Ma K.F. and Breckenridge A. (2014) Pre-aged plant waxes in tropical lake sediments and their influence on the chronology of molecular paleoclimate proxy records. *Geochim. Cosmochim. Acta* **141**, 346-364.

Drake H. and Burrows C.J. (1980) The influx of potential macrofossils into Lady Lake, north Westland, New Zealand. *N.Z.J. Bot.* **18**, 257-274.

836 Eglinton T.I., Benitez-Nelson B.C., Pearson A., McNichol A.P., Bauer J.E. and Druffel E.R.M. (1997)
837 Variability in radiocarbon ages of individual organic compounds from marine sediments. *Science*
838 **277**, 796-799.
839 Feakins S.J., Kirby M.E., Cheetham M.I., Ibarra Y. and Zimmerman S.R.H. (2014) Fluctuation in leaf
840 wax D/H ratio from a southern California lake records significant variability in isotopes in
841 precipitation during the late Holocene. *Org. Geochem.* **66**, 48-59.
842 Feng X., Benitez-Nelson B.C., Montluçon D.B., Prahl F.G., McNichol A.P., Xu L., Repeta D.J. and
843 Eglinton T.I. (2013) ^{14}C and ^{13}C characteristics of higher plant biomarkers in Washington margin
844 surface sediments. *Geochim. Cosmochim. Acta* **105**, 14-30.
845 Fox W.F. (1902) *A history of the lumber industry in the state of New York*. U.S. Dept. of Agriculture,
846 Bureau of Forestry, Washington, D.C.
847 Freimuth E.J., Diefendorf A.F. and Lowell T.V. (2017) Hydrogen isotopes of *n*-alkanes and *n*-alkanoic
848 acids as tracers of precipitation in a temperate forest and implications for paleorecords. *Geochim.*
849 *Cosmochim. Acta* **206**, 166-183.
850 Freimuth E.J., Diefendorf A.F., Lowell T.V., Bates B.R., Schartman A., Bird B.W., Landis J.D. and
851 Stewart A.K. (2020) Contrasting sensitivity of lake sediment *n*-alkanoic acids and *n*-alkanes to
852 basin-scale vegetation and regional-scale precipitation δ^2H in the Adirondack Mountains, NY
853 (USA). *Geochim. Cosmochim. Acta* **268**, 22-41.
854 Freimuth E.J., Diefendorf A.F., Lowell T.V. and Wiles G.C. (2019) Sedimentary *n*-alkanes and *n*-
855 alkanoic acids in a temperate bog are biased toward woody plants. *Org. Geochem.* **128**, 94-107.
856 French K.L., Hein C.J., Haghipour N., Wacker L., Kudrass H.R., Eglinton T.I. and Galy V. (2018)
857 Millennial soil retention of terrestrial organic matter deposited in the Bengal Fan. *Scientific*
858 *Reports* **8**, 11997.
859 Gao L., Zheng M., Fraser M. and Huang Y. (2014) Comparable hydrogen isotopic fractionation of plant
860 leaf wax *n*-alkanoic acids in arid and humid subtropical ecosystems. *Geochemistry, Geophysics,*
861 *Geosystems* **15**, 361-373.

862 Gasith A. and Hosier A.D. (1976) Airborne litterfall as a source of organic matter in lakes. *Limnol.*
863 *Oceanog.* **21**, 253-258.
864 Gierga M., Hajdas I., van Raden U.J., Gilli A., Wacker L., Sturm M., Bernasconi S.M. and Smittenberg
865 R.H. (2016) Long-stored soil carbon released by prehistoric land use: Evidence from compound-
866 specific radiocarbon analysis on Soppensee lake sediments. *Quat. Sci. Revs.* **144**, 123-131.
867 Gray A.B., Pasternack G.B. and Watson E.B. (2010) Hydrogen peroxide treatment effects on the particle
868 size distribution of alluvial and marsh sediments. *The Holocene* **20**, 293-301.
869 Greenwood D.R. (1991) The taphonomy of plant macrofossils, in: Donovan, S.K. (Ed.), The processes of
870 fossilization. Belhaven Press, Great Britain, pp. 141-169.
871 Haas M., Kaltenrieder P., Ladd S.N., Welte C., Strasser M., Eglinton T.I. and Dubois N. (2020) Land-use
872 evolution in the catchment of Lake Murten, Switzerland. *Quat. Sci. Revs.* **230**, 106154.
873 Hilton J., Lishman J.P. and Allen P.V. (1986) The dominant processes of sediment distribution and
874 focusing in a small, eutrophic, monomictic lake. *Limnol. Oceanog.* **31**, 125-133.
875 Huang Y., Bol R., Harkness D.D., Ineson P. and Eglinton G. (1996) Post-glacial variations in
876 distributions, ^{13}C and ^{14}C contents of aliphatic hydrocarbons and bulk organic matter in three
877 types of British acid upland soils. *Org. Geochem.* **24**, 273-287.
878 Huang Y., Li B., Bryant C., Bol R. and Eglinton G. (1999) Radiocarbon dating of aliphatic hydrocarbons:
879 a new approach for dating passive-fraction carbon in soil horizons. *Soil Science Society of*
880 *America Journal* **63**, 1181-1187.
881 Jackson S.T. and Whitehead D.R. (1991) Holocene Vegetation Patterns in the Adirondack Mountains.
882 *Ecology* **72**, 641-653.
883 Jordan M. and Likens G.E. (1975) An organic carbon budget for an oligotrophic lake in New Hampshire,
884 U.S.A. *SIL Proceedings, 1922-2010* **19**, 994-1003.
885 Kusch S., Rethemeyer J., Schefuß E. and Mollenhauer G. (2010) Controls on the age of vascular plant
886 biomarkers in Black Sea sediments. *Geochim. Cosmochim. Acta* **74**, 7031-7047.

887 Landis J.D., Renshaw C.E. and Kaste J.M. (2012) Measurement of ^{7}Be in soils and sediments by gamma
888 spectroscopy. *Chem. Geol.* **291**, 175-185.
889 Lane C.S., Horn S.P., Taylor Z.P. and Kerr M.T. (2016) Correlation of bulk sedimentary and compound-
890 specific δ13C values indicates minimal pre-aging of n-alkanes in a small tropical watershed.
891 *Quat. Sci. Revs.* **145**, 238-242.
892 Lavoie M., Pellerin S., Larocque M. and Bottollier-Curtet M. (2015) Late Glacial and Holocene
893 vegetation history in the northern foothills of the Adirondack Mountains. *Écoscience* **22**, 59-70.
894 Lichtfouse E., Chenu C., Baudin F., Leblond C., Da Silva M., Behar F., Derenne S., Largeau C., Wehrung
895 P. and Albrecht P. (1998a) A novel pathway of soil organic matter formation by selective
896 preservation of resistant straight-chain biopolymers: chemical and isotope evidence. *Org.*
897 *Geochem.* **28**, 411-415.
898 Lichtfouse E., Wehrung P. and Albrecht P. (1998b) Plant wax *n*-alkanes trapped in soil humin by
899 noncovalent bonds. *Naturwissenschaften* **85**, 449-452.
900 McMartin B. (1994) The great forests of the Adirondacks. North Country Books, Utica, NY. *The great*
901 *forests of the Adirondacks. North Country Books, Utica, NY.*, 240.
902 McQueen D.R. (1969) Macroscopic plant remains in Recent lake sediments. *Tuatara* **17**, 13-19.
903 Menking K.M., Peteet D.M. and Anderson R.Y. (2012) Late-glacial and Holocene vegetation and climate
904 variability, including major droughts, in the Sky Lakes region of southeastern New York State.
905 *Palaeogeography, Palaeoclimatology, Palaeoecology* **353-355**, 45-59.
906 Meyers P.A. and Kites R.A. (1982) Extractable organic compounds in midwest rain and snow. *Atmos.*
907 *Environ.* **16**, 2169-2175.
908 Millard A.R. (2014) Conventions for Reporting Radiocarbon Determinations. *Radiocarbon* **56**, 555-559.
909 Nelson D.B., Knohl A., Sachse D., Schefuß E. and Kahmen A. (2017) Sources and abundances of leaf
910 waxes in aerosols in central Europe. *Geochim. Cosmochim. Acta* **198**, 299-314.
911 Nelson D.B., Ladd S.N., Schubert C.J. and Kahmen A. (2018) Rapid atmospheric transport and large-
912 scale deposition of recently synthesized plant waxes. *Geochim. Cosmochim. Acta* **222**, 599-617.

913 Nierop K.G.J. and Buurman P. (1998) Composition of soil organic matter and its water-soluble fraction
914 under young vegetation on drift sand, central Netherlands. *European Journal of Soil Science* **49**,
915 605-615.
916 Otis M. (2018) *Rural Indigenousness: A History of Iroquoian and Algonquian Peoples of the*
917 *Adirondacks*. Syracuse University Press.
918 Overpeck J.T. (1985) A pollen study of a late Quaternary peat bog, south-central Adirondack Mountains,
919 New York. *GSA Bulletin* **96**, 145-154.
920 Pearson A. and Eglinton T.I. (2000) The origin of *n*-alkanes in Santa Monica Basin surface sediment: a
921 model based on compound-specific $\Delta^{14}C$ and $\delta^{13}C$ data. *Org. Geochem.* **31**, 1103-1116.
922 Pearson A., McNichol A.P., Benitez-Nelson B.C., Hayes J.M. and Eglinton T.I. (2001) Origins of lipid
923 biomarkers in Santa Monica Basin surface sediment: A case study using compound-specific
924 Δ14C analysis. *Geochim. Cosmochim. Acta* **65**, 3123-3137.
925 Pederson D.C., Peteet D.M., Kurdyla D. and Guilderson T. (2005) Medieval Warming, Little Ice Age,
926 and European impact on the environment during the last millennium in the lower Hudson Valley,
927 New York, USA. *Quat. Res.* **63**, 238-249.
928 PRISM (2020) PRISM Climate Group, Oregon State University, http://prism.oregonstate.edu.
929 Rach O., Brauer A., Wilkes H. and Sachse D. (2014) Delayed hydrological response to Greenland cooling
930 at the onset of the Younger Dryas in western Europe. *Nat. Geosci.* **7**, 109-112.
931 Reimer P.J., Bard E., Bayliss A., Beck J.W., Blackwell P.G., Ramsey C.B., Buck C.E., Cheng H.,
932 Edwards R.L., Friedrich M., Grootes P.M., Guilderson T.P., Haflidason H., Hajdas I., Hatté C.,
933 Heaton T.J., Hoffmann D.L., Hogg A.G., Hughen K.A., Kaiser K.F., Kromer B., Manning S.W.,
934 Niu M., Reimer R.W., Richards D.A., Scott E.M., Southon J.R., Staff R.A., Turney C.S.M. and
935 van der Plicht J. (2013) IntCal13 and Marine13 Radiocarbon Age Calibration Curves 0–50,000
936 Years cal BP. *Radiocarbon* **55**, 1869-1887.
937 Sachse D., Billault I., Bowen G.J., Chikaraishi Y., Dawson T.E., Feakins S.J., Freeman K.H., Magill
938 C.R., McInerney F.A., van der Meer M.T.J., Polissar P., Robins R.J., Sachs J.P., Schmidt H.-L.,

939 Sessions A.L., White J.W.C., West J.B. and Kahmen A. (2012) Molecular paleohydrology:
940 Interpreting the hydrogen-isotopic composition of lipid biomarkers from photosynthesizing
941 organisms. *Annu. Rev. Earth Planet. Sci.* **40**, 221-249.
942 Sachse D., Radke J. and Gleixner G. (2006) δD values of individual *n*-alkanes from terrestrial plants
943 along a climatic gradient – Implications for the sedimentary biomarker record. *Org. Geochem.* **37**,
944 469-483.
945 Schartman A.K., Diefendorf A.F., Lowell T.V., Freimuth E.J., Stewart A.K., Landis J.D. and Bates B.R.
946 (2020) Stable source of Holocene spring precipitation recorded in leaf wax hydrogen-isotope
947 ratios from two New York lakes. *Quat. Sci. Revs.* **240**, 106357.
948 Schefuß E., Eglinton T.I., Spencer-Jones C.L., Rullkötter J., De Pol-Holz R., Talbot H.M., Grootes P.M.
949 and Schneider R.R. (2016) Hydrologic control of carbon cycling and aged carbon discharge in the
950 Congo River basin. *Nat. Geosci.* **9**, 687-690.
951 Smittenberg R.H., Eglinton T.I., Schouten S. and Damsté J.S.S. (2006) Ongoing Buildup of Refractory
952 Organic Carbon in Boreal Soils During the Holocene. *Science* **314**, 1283-1286.
953 Smittenberg R.H., Hopmans E.C., Schouten S., Hayes J.M., Eglinton T.I. and Sinninghe Damsté J.S.
954 (2004) Compound-specific radiocarbon dating of the varved Holocene sedimentary record of
955 Saanich Inlet, Canada. *Paleoceanography* **19**, PA2012.
956 Spicer R.A. and Wolfe A.P. (1987) Plant taphonomy of late Holocene deposits in Trinity (Clair Engle)
957 Lake, northern California. *Paleobiology* **13**, 227-245.
958 Stuiver M. and Polach H.A. (1977) Discussion Reporting of ^{14}C Data. *Radiocarbon* **19**, 355-363.
959 Stuiver M. and Reimer P.J. (1993) Extended ^{14}C Data Base and Revised CALIB 3.0 ^{14}C Age Calibration
960 Program. *Radiocarbon* **35**, 215-230.
961 Uchikawa J., Popp B.N., Schoonmaker J.E. and Xu L. (2008) Direct application of compound-specific
962 radiocarbon analysis of leaf waxes to establish lacustrine sediment chronology. *J. Paleolimnol.*
963 **39**, 43-60.

van der Voort T.S., Zell C.I., Hagedorn F., Feng X., McIntyre C.P., Haghipour N., Graf Pannatier E. and Eglinton T.I. (2017) Diverse soil carbon dynamics expressed at the molecular level. *Geophysical Research Letters* **44**, 11,840-811,850.

Vonk J.E., Drenzek N.J., Hughen K.A., Stanley R.H.R., McIntyre C., Montluçon D.B., Giosan L., Southon J.R., Santos G.M., Druffel E.R.M., Andersson A.A., Sköld M. and Eglinton T.I. (2019) Temporal deconvolution of vascular plant-derived fatty acids exported from terrestrial watersheds. *Geochim. Cosmochim. Acta* **244**, 502-521.

Vonk J.E., van Dongen B.E. and Gustafsson Ö. (2010) Selective preservation of old organic carbon fluvially released from sub-Arctic soils. *Geophysical Research Letters* **37**, n/a-n/a.

Whitehead D.R., Charles D.F., Jackson S.T., Smol J.P. and Engstrom D.R. (1989) The developmental history of Adirondack (N.Y.) lakes. *J. Paleolimnol.* **2**, 185-206.

Whitehead D.R. and Jackson S. (1990) The regional vegetational history of the High Peaks (Adirondack Mountains). *New York. New York State Museum and Science Service Bulletin* **478**.

Table 1
Lake locations and basin details.

				Lake basin		Drainage basin					
Lake	Latitude (ºN)	Longitude (ºE)	Elevation (m)	Depth max. (m)	Area (km^2)	Area (km^2)	Lake area (%)	Relief (m)	Inlets	Outlets	Soil B-horizon Max. Depth (cm)
Debar Pond	44.62189	-74.19359	478	10.0	0.35	6.33	5.5	440	5	1	35-99
East Pine Pond	44.33827	-74.41497	486	10.1	0.27	0.66	40.2	24	0	1	81
Heart Lake	44.18251	-73.96928	666	13.6	0.11	0.63	17.7	220	0	1	86
Moose Pond	44.37172	-74.06197	474	21.3	0.64	17.70	3.6	692	2	1	35-86
Wolf Pond	44.01785	-74.22170	558	12.0	0.57	6.48	8.8	258	3	1	23-86

Table 2
Radiocarbon macrofossil sample information for each of the five lakes. Ages were used along with ^{210}Pb ages to constrain sediment age using BACON. The National Ocean Sciences Accelerator Mass Spectrometry (NOSAMS) accession numbers are provided.

Lake	Depth (cm)	Accession number	Age (^{14}C yr BP)	1σ
Debar Pond	130	OS-137958	330	15
East Pine Pond	110.25	OS-134713	1,400	25
	407	OS-138208	4,670	25
	580	OS-137961	6,860	30
Heart Lake	145	OS-134712	675	20
	298	OS-137959	2,950	20
	358	OS-138210	3,910	30
	418	OS-137960	4,790	25
	598	OS-138207	8,130	45
Moose Pond	121.25	OS-134714	1,500	20
	431	OS-138209	5,770	30
	530.5	OS-138214	8,030	40
	684	OS-138211	11,200	70
Wolf Pond	137.25	OS-141050	1,270	15
	143	OS-141049	1,090	15

Figure 1

Click here to access/download;Figure;Figure 1 Overview map.pdf

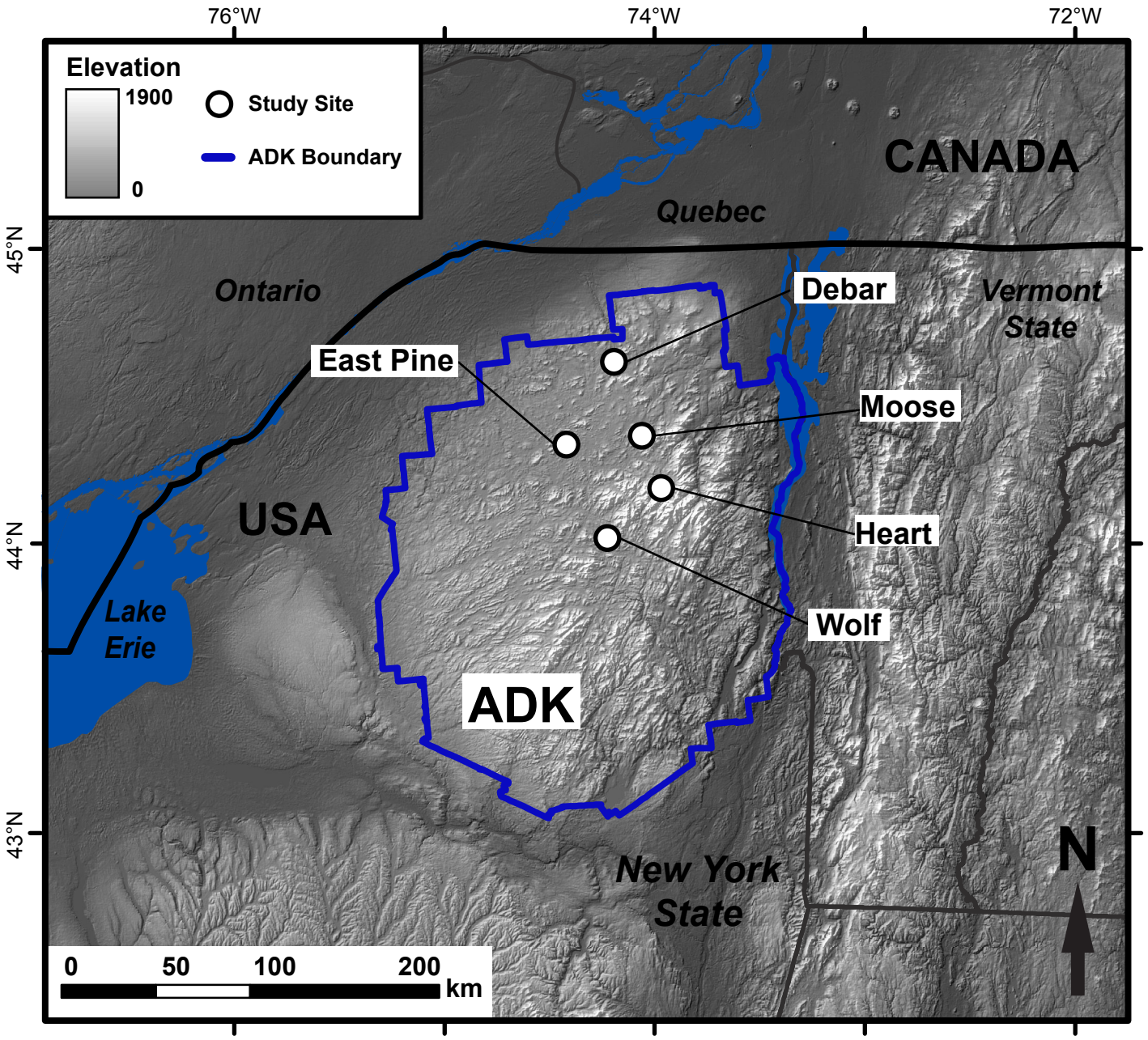

Figure 2

Click here to access/download;Figure;Figure 2 Basins reduced.pdf

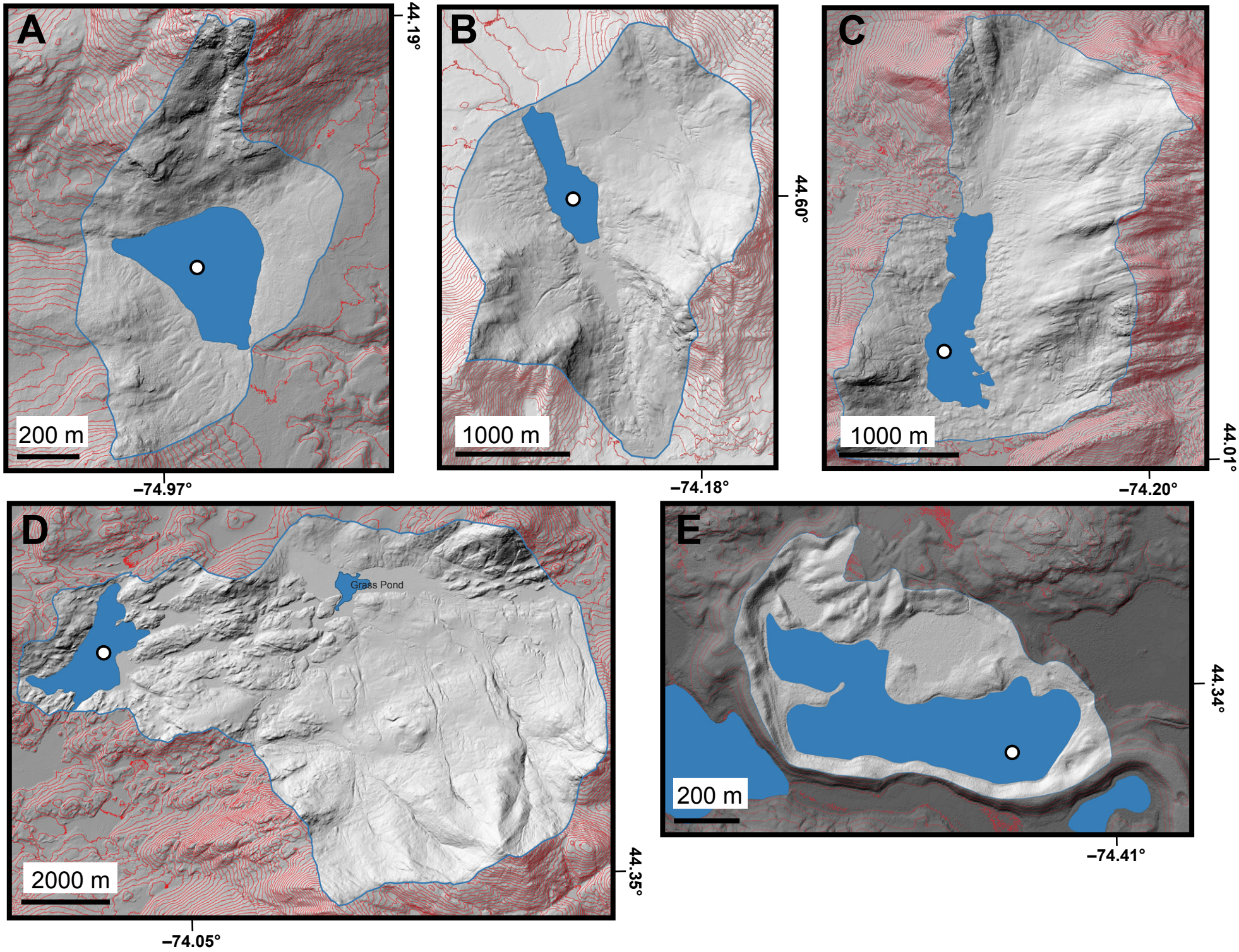

Figure 3

Click here to access/download;Figure;Figure 3 Age models R1.pdf

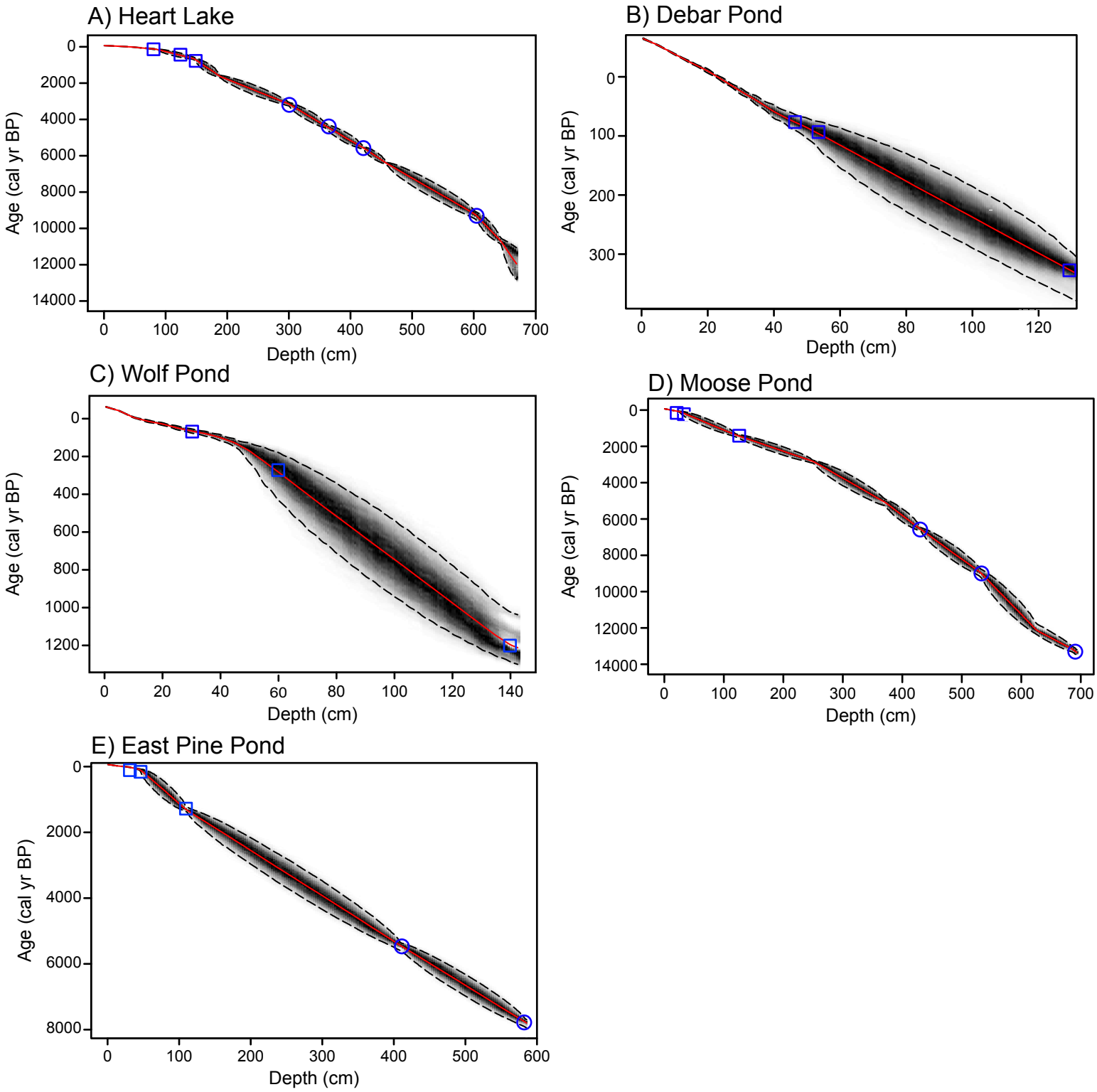

Figure 4

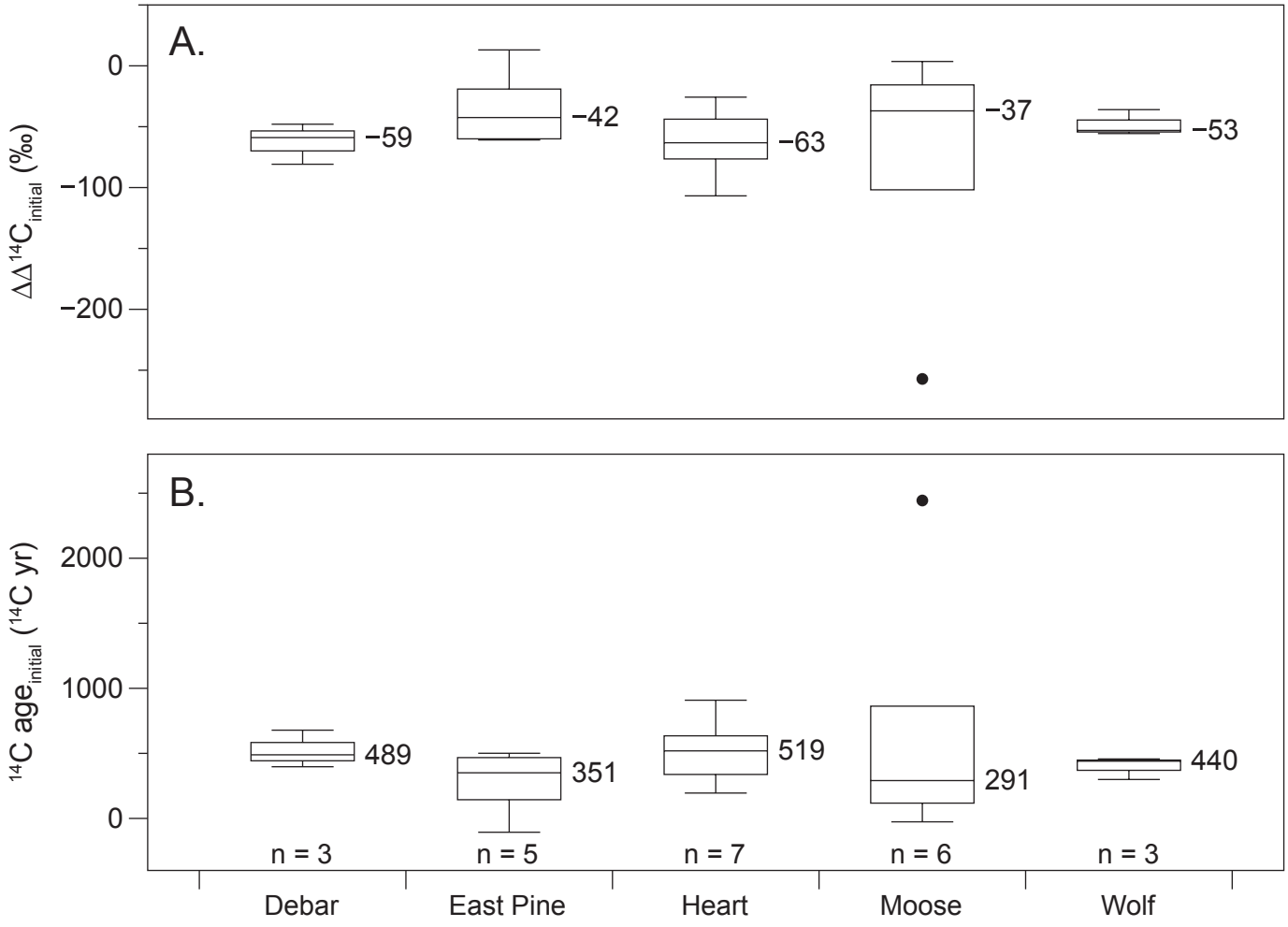

Figure 5

Click here to access/download;Figure;Figure 5 n-Alkane age offsets.pdf

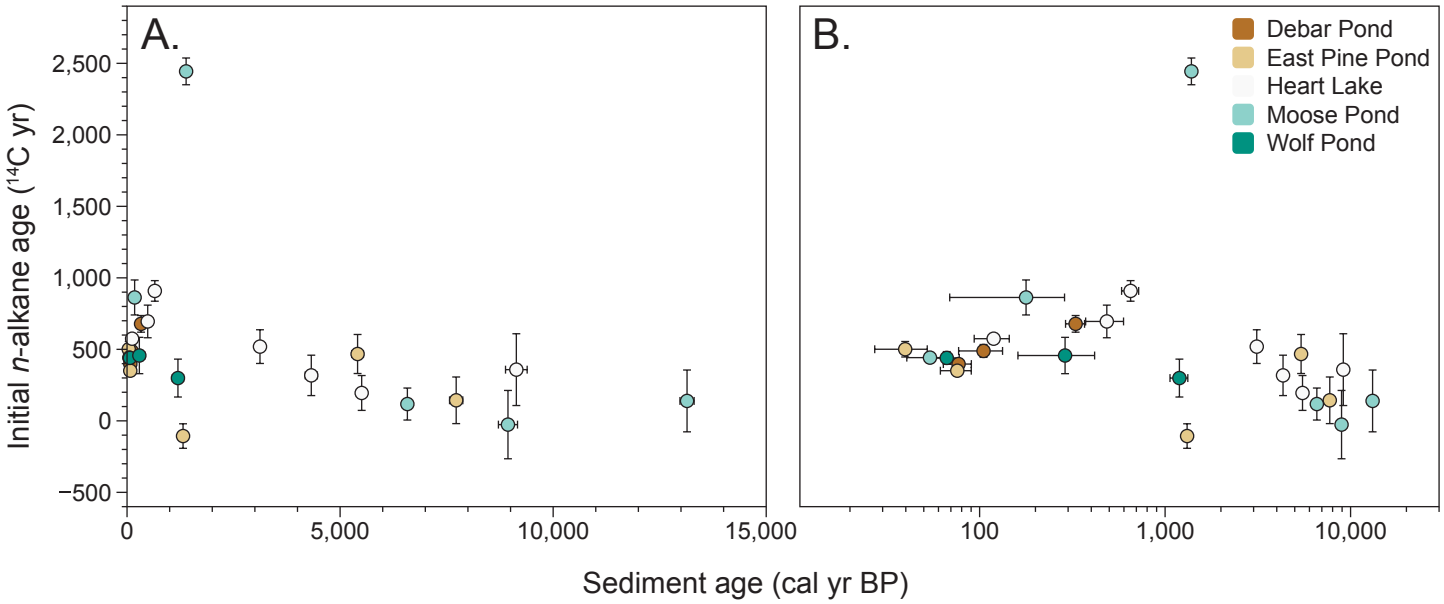

Figure 6

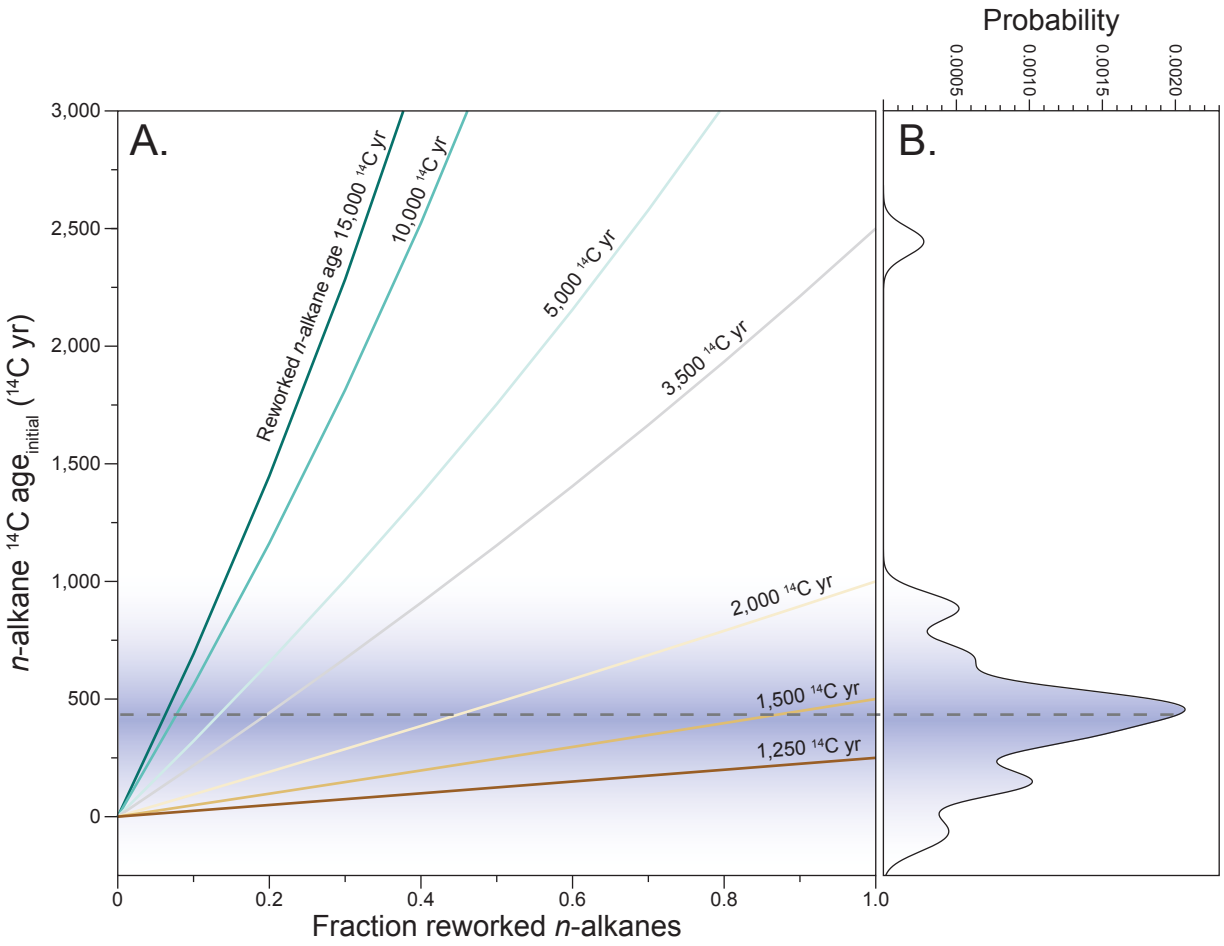

Highlights

1. Five lake sediment records in the Adirondacks region of New York (USA) were studied

2. Plant wax *n*-alkane ^{14}C ages at the time of sediment deposition were determined

3. The average *n*-alkane ^{14}C $age_{initial}$ for all lakes was 400 ^{14}C yr

4. The age of *n*-alkanes were almost always older (offset) than the age of the sediments

5. Age offsets are caused by sediment focusing and reworking of soil-derived *n*-alkanes